

SUPPORTING INFORMATION

Rule Breaker Boron Clusters: A New Class of Hypoelectronic Osmaborane Clusters $[(\text{Cp}^*\text{Os})_2\text{B}_n\text{H}_n]$ ($n = 6-10$)

*Ketaki Kar, Sourav Kar and Sundargopal Ghosh**

Department of Chemistry, Indian Institute of Technology Madras, Chennai 600036, India. Tel: +91 44-22574230; E-mail: sghosh@iitm.ac.in

Table of contents

I Experimental Details

I.1 Supplementary Data

Figure S1 Molecular structure and labeling diagram of **1**.

Figure S2 Molecular structure and labeling diagram of **2**.

Figure S3 Molecular structure and labeling diagram of **3**.

Figure S4 Molecular structure and labeling diagram of **4**.

Figure S5 Molecular structure and labeling diagram of **5**.

I.2 Spectroscopic Details

Figure S6 ESI-MS spectrum of **1**.

Figure S7 ^1H NMR spectrum of **1** in CDCl_3 .

Figure S8 Stacked ^1H (blue) and $^1\text{H}\{^{11}\text{B}\}$ (red) NMR spectra of **1** in CDCl_3 .

Figure S9 $^{11}\text{B}\{^1\text{H}\}$ NMR spectrum of **1** in CDCl_3 .

Figure S10 $^{13}\text{C}\{^1\text{H}\}$ NMR spectrum of **1** in CDCl_3 .

Figure S11 IR spectrum of **1**.

Figure S12 ESI-MS spectrum of **2**

Figure S13 ^1H NMR spectrum of **2** in CDCl_3 .

Figure S14 Stacked ^1H (blue) and $^1\text{H}\{^{11}\text{B}\}$ (red) NMR spectra of **2** in CDCl_3 .

Figure S15 $^{11}\text{B}\{^1\text{H}\}$ NMR spectrum of **2** in CDCl_3 .

Figure S16 $^{13}\text{C}\{^1\text{H}\}$ NMR spectrum of **2** in CDCl_3 .

Figure S17 IR spectrum of **2**.

Figure S18 ESI-MS spectrum of **3**

Figure S19 ^1H NMR spectrum of **3** in CDCl_3 .

Figure S20 $^{11}\text{B}\{^1\text{H}\}$ NMR spectrum of **3** in CDCl_3 .

Figure S21 $^{13}\text{C}\{^1\text{H}\}$ NMR spectrum of **3** in CDCl_3 .

Figure S22 IR spectrum of **3**

Figure S23 ESI-MS spectrum of **4**

Figure S24 ^1H NMR spectrum of **4** in CDCl_3 .

Figure S25 Stacked ^1H (blue) and $^1\text{H}\{^{11}\text{B}\}$ (red) NMR spectra of **4** in CDCl_3 .

Figure S26 $^{11}\text{B}\{^1\text{H}\}$ NMR spectrum of **4** in CDCl_3 .

- Figure S27 $^{13}\text{C}\{^1\text{H}\}$ NMR spectrum of **4** in CDCl_3 .
- Figure S28 IR spectrum of **4**.
- Figure S29 ESI-MS spectrum of **5**
- Figure S30 ^1H NMR spectrum of **5** in CDCl_3 .
- Figure S31 $^{11}\text{B}\{^1\text{H}\}$ NMR spectrum of **5** in CDCl_3 .
- Figure S32 $^{13}\text{C}\{^1\text{H}\}$ NMR spectrum of **5** in CDCl_3 .
- Figure S33 IR spectrum of **5**.
- Figure S34 UV-Vis spectra of **1-5**.

I.3 X-ray Analysis Details

II Computational Details

- Table S1 Bond parameters of clusters **1-5** are compared with their optimized values and WBIs.
- Figure S35 Selected molecular orbitals of cluster **1**.
- Figure S36 Selected molecular orbitals of cluster **2**.
- Figure S37 Selected molecular orbitals of cluster **3**.
- Figure S38 Selected molecular orbitals of cluster **4**.
- Figure S39 Selected molecular orbitals of cluster **5**.
- Table S2 Calculated natural charges (q_{Os} , and q_{B}), natural valence populations (Pop) and HOMO–LUMO gaps ($\Delta E_{\text{H-L}}$) of clusters **1-5**.
- Figure S40 Calculated absorption spectrum of **1**.
- Table S3 TD-DFT calculated electronic transition configuration for **1** along with their corresponding excitation energies, wavelength and oscillator strengths.
- Figure S41 Calculated absorption spectrum of **2**.
- Table S4 TD-DFT calculated electronic transition configuration for **2** along with their corresponding excitation energies, wavelength and oscillator strengths.
- Figure S42 Calculated absorption spectrum of **3**.
- Table S5 TD-DFT calculated electronic transition configuration for **3** along with their corresponding excitation energies, wavelength and oscillator strengths.
- Figure S43 Calculated absorption spectrum of **4**.
- Table S6 TD-DFT calculated electronic transition configuration for **4** along with their corresponding excitation energies, wavelength and oscillator strengths.

Figure S44 Calculated absorption spectrum of **5**.

Table S7 TD-DFT calculated electronic transition configuration for **5** along with their corresponding excitation energies, wavelength and oscillator strengths.

III Cartesian Coordinates of all Optimized Structures

Figure S45 Optimized geometry of **1**.

Figure S46 Optimized geometry of **2**.

Figure S47 Optimized geometry of **3**.

Figure S48 Optimized geometry of **4**.

Figure S49 Optimized geometry of **5**.

IV References

I Experimental Details

General Procedures and Instrumentation

All the manipulations were conducted under an Ar atmosphere using standard Schlenk line techniques or in a glove box. Solvents were distilled prior to use under an Ar atmosphere. LiBH_4 (2.0 M in THF) and $[\text{BH}_3\cdot\text{SMe}_2]$ were used as received (Sigma Aldrich). $[\text{Cp}^*\text{OsBr}_2]_2$ ¹ was synthesized according to the literature method. Thin layer chromatography was carried out on 250- μm diameter aluminum- supported silica gel TLC plates (MERCK TLC Plates) to separate the reaction mixtures. NMR spectra were recorded by using 400 and 500 MHz Bruker FT-NMR spectrometers. The residual solvent protons were used as reference (CDCl_3 , $\delta = 7.26$ ppm; Benzene- d_6 , $\delta = 7.16$ ppm). The inverse-gated decoupling (zgig) and power-gated (zgpr) pulse sequences, respectively, were used to get the $^{11}\text{B}\{^1\text{H}\}$ and $^1\text{H}\{^{11}\text{B}\}$ spectra. ^1H decoupled ^{11}B spectra were processed with a backward linear prediction algorithm to remove the broad ^{11}B background signal of the NMR probe and NMR tube². The mass spectra were recorded on a Bruker MicroTOF-II Qtof and 6545 Qtof LC/MS instruments. The IR spectra were recorded on a JASCO 400 FT-IR spectrometer. UV-vis absorption spectra were recorded on a Thermo Scientific (Evolution 300) UV-vis spectrometer.

Synthesis of $[(\text{Cp}^*\text{Os})_2\text{B}_6\text{H}_6]$ (1**):** Under an Ar atmosphere, in a flame-dried Schlenk tube $[\text{Cp}^*\text{OsBr}_2]_2$ (0.1 g, 0.102 mmol) was suspended in xylene (15 mL) and cooled to -78°C . $[\text{LiBH}_4\cdot\text{THF}]$ (0.2 mL, 0.400 mmol) was added, and the reaction mixture was allowed to warm slowly to room temperature and kept stirring for another 45 mins. $[\text{BH}_3\cdot\text{THF}]$ (1 mL) was added to the reaction mixture, and the resultant mixture was slowly warmed to room temperature, allowed to stir for additional 30 min, and kept for thermolysis at 110°C for 16 h. The solvent was then removed under vacuum, and the residue was dissolved in hexane/ CH_2Cl_2 mixture (80:20) and passed via celite. The solvent was again evaporated under vacuum, and the residue was purified using silica-gel TLC plates by eluting with hexane/ CH_2Cl_2 (80:20) mixture that yielded colourless solid **1** (0.013g, 18%).

1: MS (ESI⁺): m/z calculated for $[\text{C}_{20}\text{H}_{36}\text{B}_6\text{Os}_2 + \text{Na}]^+$: 745.2505, found: 745.2463; ^1H NMR (500 MHz, CDCl_3 , 22°C): $\delta = 9.92$ (q, 2H, B- H_t), 8.97 (br, 2H, B- H_t), -2.31 (q, 2H, B- H_t), 2.03 (s, 30H, $2\times\text{Cp}^*$); $^1\text{H}\{^{11}\text{B}\}$ NMR (500 MHz, CDCl_3 , 22°C): δ (ppm) = 9.92 (q, 2H, B- H_t), 8.97 (br, 2H, B- H_t) -2.31 (s, 2H, B- H_t); $^{11}\text{B}\{^1\text{H}\}$ NMR (160 MHz, CDCl_3 , 22°C): δ (ppm) = 97.4 (s, 2B), 61.3 (s, 2B), -

16.3 (s, 2B); $^{13}\text{C}\{^1\text{H}\}$ NMR (125 MHz, CDCl_3 , 22 °C): δ (ppm) = 95.8 (C_5Me_5), 11.2 (C_5Me_5); IR (dichloromethane, cm^{-1}): $\bar{\nu}$ = 2530 (B- H_t), 2500 (B- H_t).

Synthesis of $[(\text{Cp}^*\text{Os})_2\text{B}_7\text{H}_7]$ (2), $[(\text{Cp}^*\text{Os})_2\text{B}_8\text{H}_8]$ (3) and $[(\text{Cp}^*\text{Os})_2\text{B}_9\text{H}_9]$ (4): Under an Ar atmosphere, in a moisture-free Schlenk tube, $[\text{Cp}^*\text{OsBr}_2]_2$ (0.1 g, 0.102 mmol) was suspended in 15 mL toluene and cooled to -78°C . $[\text{LiBH}_4\cdot\text{THF}]$ (0.2 mL, 0.400 mmol) was added dropwise, and the reaction mixture was allowed to warm slowly to room temperature and kept stirring for another 45 mins. $[\text{BH}_3\cdot\text{SMe}_2]$ (1 mL) was added to the reaction mixture, and the resultant mixture was slowly warmed to room temperature, allowed to stir for additional 30 min, and kept for thermolysis at 90°C for 17 h. The solvent was then removed under vacuum, and the residue was dissolved in hexane/ CH_2Cl_2 mixture (60:40) and passed via celite. The solvent was again evaporated under vacuum, and the residue was purified using silica-gel TLC plates by eluting with hexane/ CH_2Cl_2 (60:40) mixture that yielded dark green solid **2** (0.009g, 12%), orange solid **3** (0.005g, 7%), violet solid **4** (0.008g, 10%) compounds.

2: MS (ESI⁺): m/z calculated for $[\text{C}_{20}\text{H}_{37}\text{B}_7\text{Os}_2 + \text{H}]^+$: 735.2865, found: 735.2891; ^1H NMR (500 MHz, CDCl_3 , 22 °C): δ = 10.71 (br, 1H, B- H_t), 8.70 (q, 4H, B- H_t), 1.96 (s, 30H, $2\times\text{Cp}^*$); $^1\text{H}\{^{11}\text{B}\}$ NMR (500 MHz, CDCl_3 , 22 °C): δ (ppm) = 10.71 (br, 1H, B- H_t), 8.70 (q, 4H, B- H_t), 0.17 (br, 2H, B- H_t), 1.96 (s, 30H, $2\times\text{Cp}^*$); $^{11}\text{B}\{^1\text{H}\}$ NMR (160 MHz, CDCl_3 , 22 °C): δ (ppm) = 107.7 (s, 1B), 77.7 (s, 1B), 61.2 (s, 2B), 56.0 (s, 2B), 6.2 (s, 1B); $^{13}\text{C}\{^1\text{H}\}$ NMR (125 MHz, CDCl_3 , 22 °C): δ (ppm) = 96.3 (C_5Me_5), 10.8 (C_5Me_5); IR (dichloromethane, cm^{-1}): $\bar{\nu}$ = 2500 (B- H_t), 2440 (B- H_t).

3: MS (ESI⁺): m/z calculated for $[\text{C}_{20}\text{H}_{38}\text{B}_8\text{Os}_2 + \text{K}]^+$: 784.2600, found: 784.3152; ^1H NMR (500 MHz, CDCl_3 , 22 °C): δ = 11.29 (q, B- H_t), 9.09 (q, B- H_t), 6.54 (br, B- H_t), 1.97 (s, 15H; $1\times\text{Cp}^*$), 1.79 (s, 15H; $1\times\text{Cp}^*$); $^{11}\text{B}\{^1\text{H}\}$ NMR (160 MHz, CDCl_3 , 22 °C): δ (ppm) = 89.3 (br, 1B), 79.5 (br, 1B), 78.8 (br, 1B), 22.1 (br, 1B), 20.8 (br, 1B), 14.0 (br, 1B), -12.3 (br, 1B), -13.0 (br, 1B); $^{13}\text{C}\{^1\text{H}\}$ NMR (125 MHz, CDCl_3 , 22 °C): δ (ppm) = 99.1, 97.5 (C_5Me_5), 10.3, 9.5 (C_5Me_5); IR (dichloromethane, cm^{-1}): $\bar{\nu}$ = 2518 (B- H_t), 2475 (B- H_t).

4: MS (ESI⁺): m/z calculated for $[\text{C}_{20}\text{H}_{39}\text{B}_9\text{Os}_2 + \text{CH}_3\text{OH}]^+$: 789.3408, found: 789.3471; ^1H NMR (500 MHz, CDCl_3 , 22 °C): δ = 11.76 (br, B- H_t), 9.69 (pcq, B- H_t), 5.03 (q, B- H_t), 3.95 (br, B- H_t), 1.84 (s, 15H, $1\times\text{Cp}^*$), 1.82 (s, 15H, $1\times\text{Cp}^*$); $^1\text{H}\{^{11}\text{B}\}$ NMR (500 MHz, CDCl_3 , 22 °C): δ (ppm) = 11.76 (br, 2H, B- H_t), 9.69 (br, 2H, B- H_t), 5.03 (br, 1H, B- H_t), 4.95 (br, 1H, B- H_t), 3.81 (br, 1H, B- H_t), 3.56 (br, 1H, B- H_t), 3.15 (br, 1H, B- H_t); $^{11}\text{B}\{^1\text{H}\}$ NMR (160 MHz, CDCl_3 , 22 °C): δ (ppm) =

95.9 (br, 1B), 79.4 (br, 1B), 23.9 (br, 1B), 18.3 (br, 1B), 11.6 (br, 1B), 8.7 (br, 1B), 6.0 (br, 1B), 3.8 (br, 1B), 2.4 (br, 1B); $^{13}\text{C}\{^1\text{H}\}$ NMR (125 MHz, CDCl_3 , 22 °C): δ (ppm) = 95.7, 94.0 (C_5Me_5), 10.3, 10.2 (C_5Me_5); IR (dichloromethane, cm^{-1}): $\bar{\nu}$ = 2526 (B- H_t), 2492 (B- H_t).

Synthesis of [(Cp*Os) $_2$ B $_{10}$ H $_{10}$] (5): Under an Ar atmosphere, in a moisture-free Schlenk tube, $[\text{Cp}^*\text{OsBr}_2]_2$ (0.1 g, 0.102 mmol) was suspended in 15 mL toluene and cooled to -78°C. $[\text{LiBH}_4\cdot\text{THF}]$ (0.2 mL, 0.400 mmol) was added dropwise, and the reaction mixture was allowed to warm slowly to room temperature and kept stirring for another 45 mins. $[\text{BH}_3\cdot\text{SMe}_2]$ (1 mL) was added to the reaction mixture, and the resultant mixture was slowly warmed to room temperature, allowed to stir for additional 30 min, and kept for reflux at 110 °C for 17 h. The solvent was then removed under vacuum, and the residue was dissolved in hexane/ CH_2Cl_2 mixture (50:50) and passed via celite. The solvent was again evaporated under vacuum, and the residue was purified using silica-gel TLC plates by eluting with hexane/ CH_2Cl_2 (50:50) mixture that yielded green solid **5** (0.004g, 5%) along with compounds **2-4** in low yields.

5: MS (ESI $^+$): m/z calculated for $[\text{C}_{20}\text{H}_{40}\text{B}_{10}\text{Os}_2 + \text{H}]^+$: 770.3404, found: 770.3433; ^1H NMR (500 MHz, CDCl_3 , 22 °C): δ (ppm) = 10.74 (br, 2H, B- H_t), 9.53 (pcq, 8H, B- H_t), 1.93 (s, 30H, 1 \times Cp*); $^{11}\text{B}\{^1\text{H}\}$ NMR (160 MHz, CDCl_3 , 22 °C): δ (ppm) = 43.9 (br, 2B), 16.1 (br, 2B), 4.6 (br, 4B), -8.7 (br, 4B); $^{13}\text{C}\{^1\text{H}\}$ NMR (125 MHz, CDCl_3 , 22 °C): δ (ppm) = 98.8 (C_5Me_5), 9.1 (C_5Me_5); IR (dichloromethane, cm^{-1}): $\bar{\nu}$ = 2492 (B- H_t), 2440 (B- H_t).

I.1 Supplementary Data

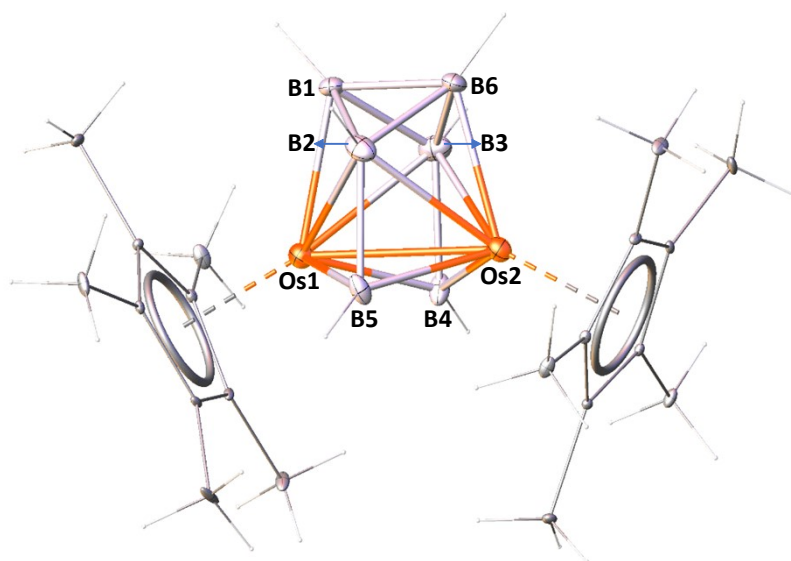


Figure S1. Molecular structure and labelling diagram of $[(\text{Cp}^*\text{Os})_2\text{B}_6\text{H}_6]$ (**1**). Selected bond lengths [\AA] and angles (deg) of **1**: Os1-Os2 2.7688(3), Os1-B4 2.055(8), Os1-B5 2.060(7), Os2-B4 2.062(7), Os2-B5 2.084(8), Os1-B1 2.134(8), Os2-B6 2.234(11); B4-Os1-Os2 47.9(2), B5-Os1-Os2 48.5(2), Os1-B4-Os2 84.5(3), Os1-B5-Os2 83.8(3), B5-Os2-Os1 47.7(2).

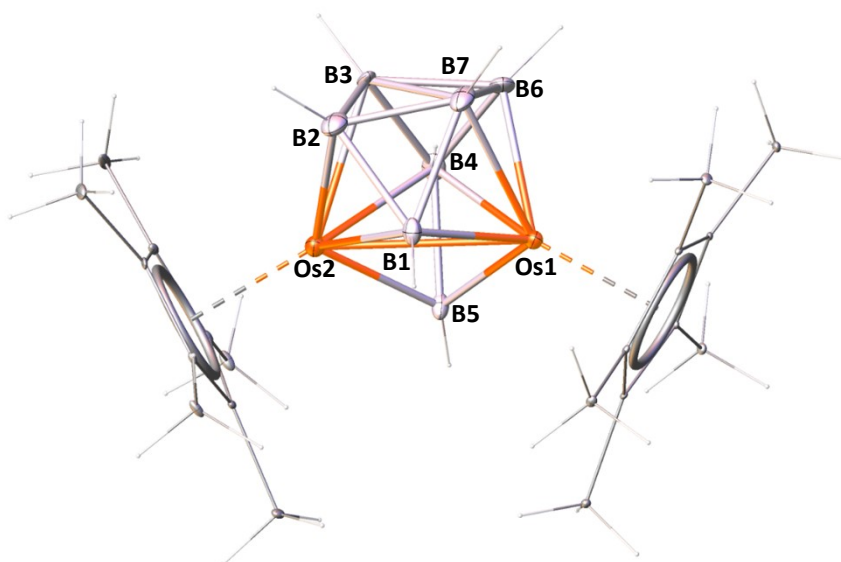


Figure S2. Molecular structure and labelling diagram of $[(\text{Cp}^*\text{Os})_2\text{B}_7\text{H}_7]$ (**2**). Selected bond lengths [\AA] and angles (deg) of **2**: B1-Os1 2.081(12), B1-Os2 2.180(11), B5-Os1 2.030(11), B5-Os2 2.040(12), B2-Os2 2.121(15), B6-Os1 2.091(13), B4-Os2 2.179(13), B4-Os1 2.236(14), B3-Os2 2.222(12), B7-Os1 2.246(13), Os2-Os1 2.805; B5-Os1-B1 93.2(5), B1-Os1-Os2 50.4(3), B5-Os1-Os2 46.6(3), B5-Os2-B1 90.1(4), B5-Os2-Os1 46.3(3), Os1-B1-Os2 82.3(4).

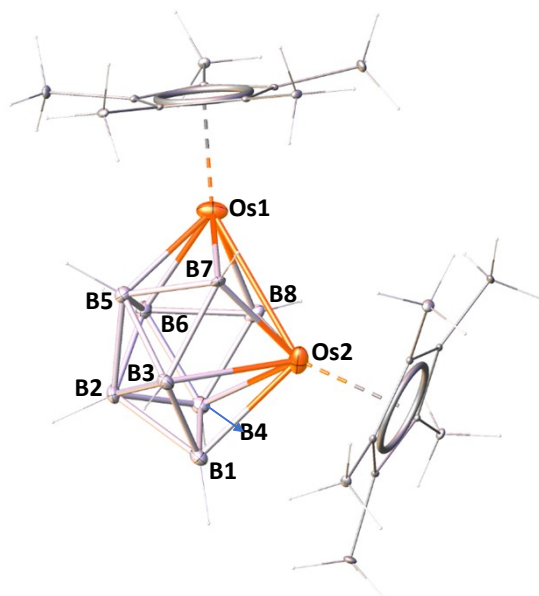


Figure S3. Molecular structure and labelling diagram of $[(\text{Cp}^*\text{Os})_2\text{B}_8\text{H}_8]$ (**3**). Selected bond lengths [\AA] and angles (deg) of **3**: Os1-Os2 2.905, Os1-B8 2.13(3), Os1-B7 2.22(4), Os2-B7 2.16(3), Os2-B8 2.14(3), Os2-B1 2.28(3), Os1-B5 2.14(4), B2-B5 1.78(5); B8-Os1-B7 91.6(12), B8-Os2-B7 93.0(13), Os2-B7-Os1 83.1(14), B7-Os2-B1 92.9(14), B8-Os1-B5 85.0(14).

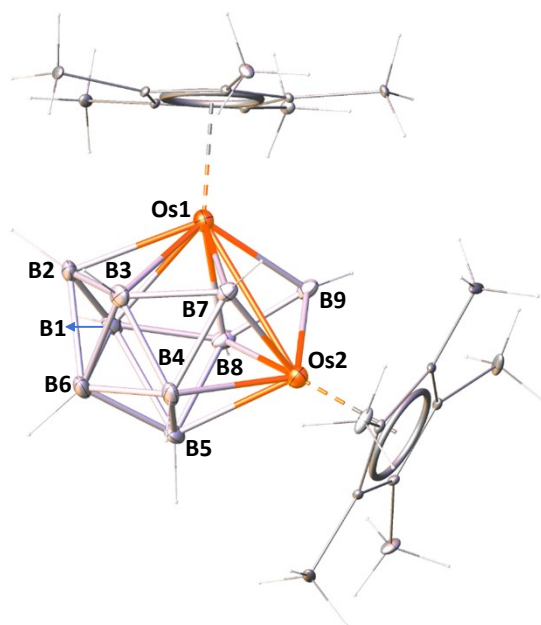


Figure S4. Molecular structure and labelling diagram of $[(\text{Cp}^*\text{Os})_2\text{B}_9\text{H}_9]$ (**4**). Selected bond lengths [\AA] and angles (deg) of **4**: Os1-B7 2.159(17), Os1-B9 2.175(17), Os2-B9 2.051(18), Os2-B7 2.138(17), Os1-B8 2.210(19), Os2-B8 2.13(2), Os1-B2 2.229(18), Os2-B5 2.212(19), B2-B6 1.82(3); B7-Os1-B9 91.4(7); B9-Os1-B8 40.4(8), B9-Os2-B7 95.5(7), B7-Os1-Os2 48.1(5), B9-Os1-Os2 45.8(5), B9-Os2-Os1 49.4(5).

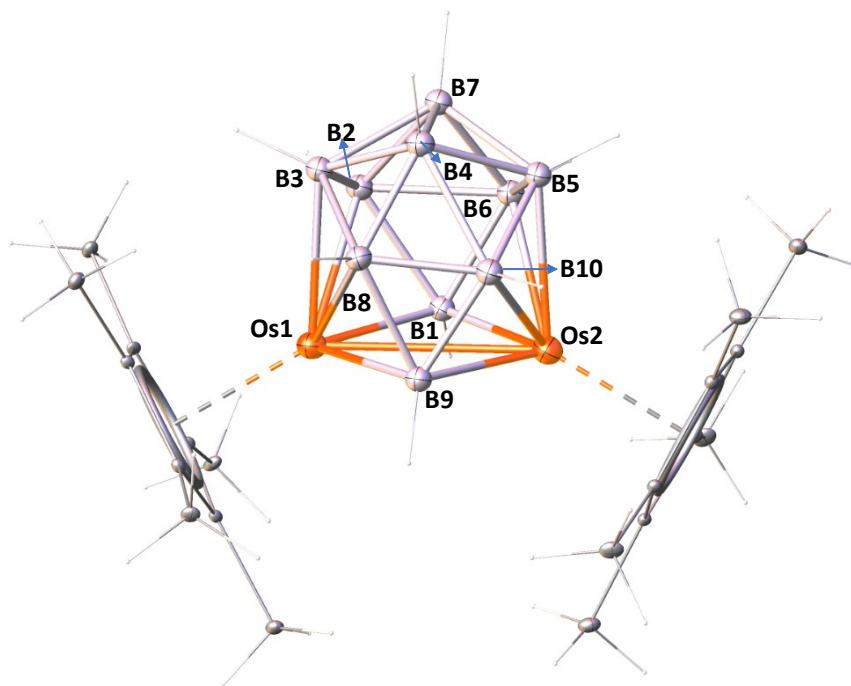


Figure S5. Molecular structure and labelling diagram of $[(\text{Cp}^*\text{Os})_2\text{B}_{10}\text{H}_{10}]$ (**5**). Selected bond lengths [\AA] and angles (deg) of **5**: Os1-Os2 2.832(2), B1-Os1 2.14(4), B2-Os1 2.20(4), B9-Os1 2.19(4), B9-Os2 2.16(4), B3-Os1 2.22(4), B5-Os2 2.20(4), B2-Os1 2.20(4), B6-Os2 2.24(4), B8-B10 1.58(5), B2-B6 1.79(6); Os2-B9-Os1 81.3(15), B9-Os2-Os1 49.9(11), B1-Os2-Os1 48.6(10), B1-Os2-B6 45.3(14), B10-Os2-B5 47.6(15), B8-Os1-Os2 73.1(9), B1-Os2-B9 98.4(15).

I.2 Spectroscopic details

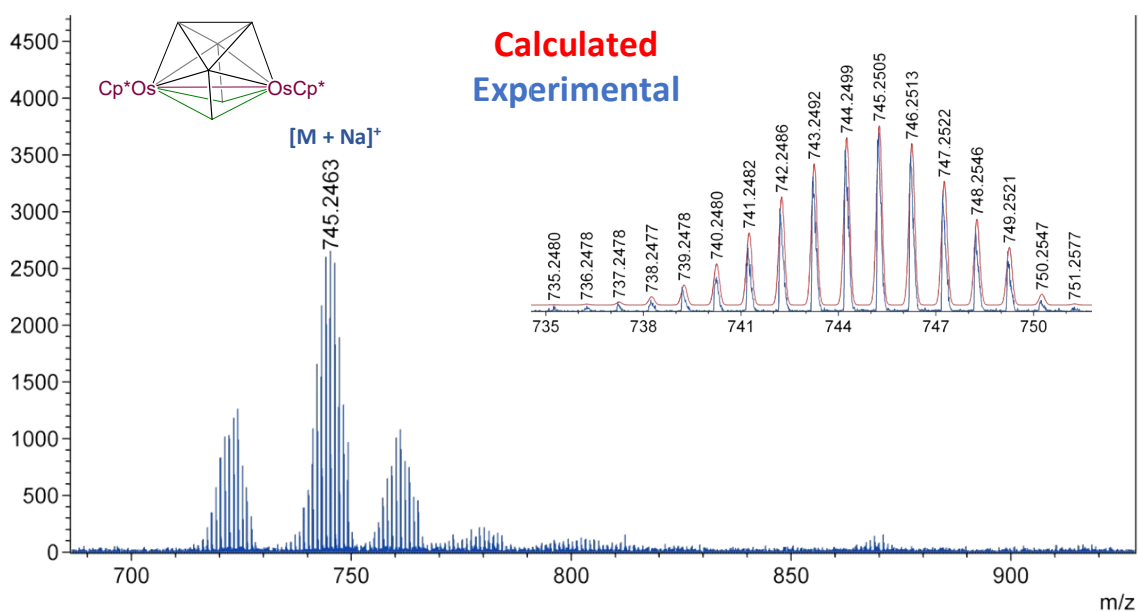


Figure S6. ESI-MS spectrum of **1**.

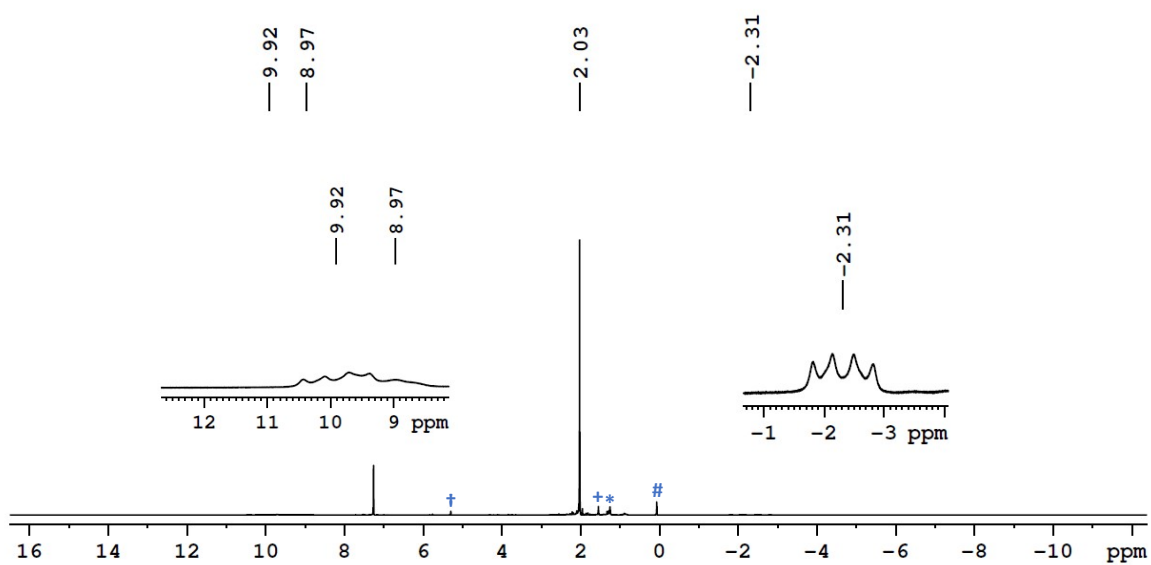


Figure S7. ^1H NMR spectrum of **1** in CDCl_3 . (#Silicon grease, † CH_2Cl_2 , ‡ H_2O , *Hexane)

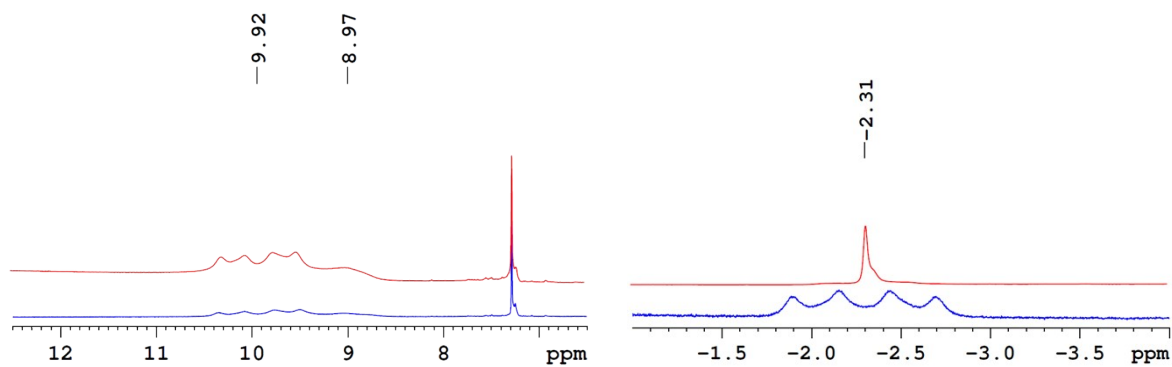


Figure S8. Stacked ^1H (blue) and $^1\text{H}\{^{11}\text{B}\}$ (red) NMR spectra of **1** in CDCl_3 .

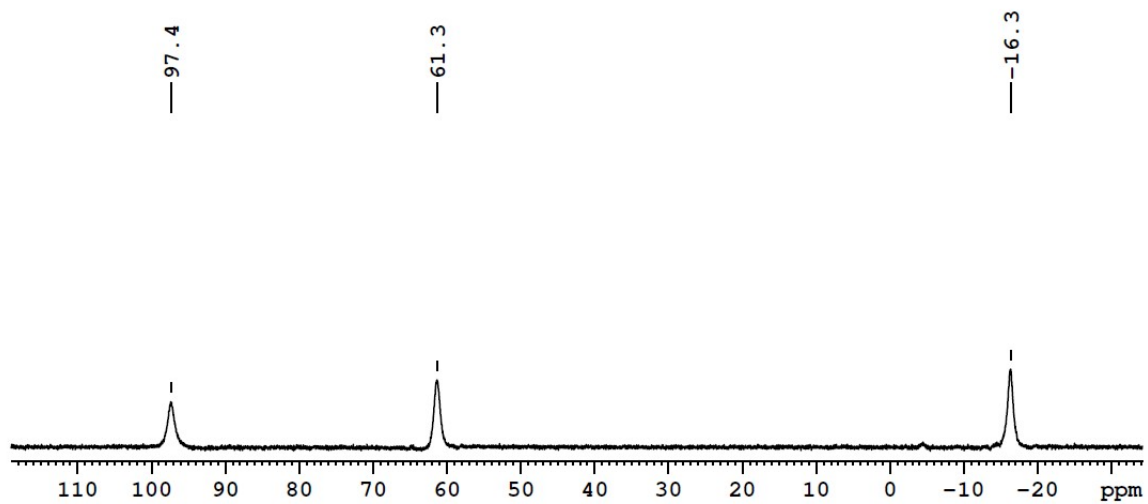


Figure S9. $^{11}\text{B}\{^1\text{H}\}$ NMR spectrum of **1** in CDCl_3 .

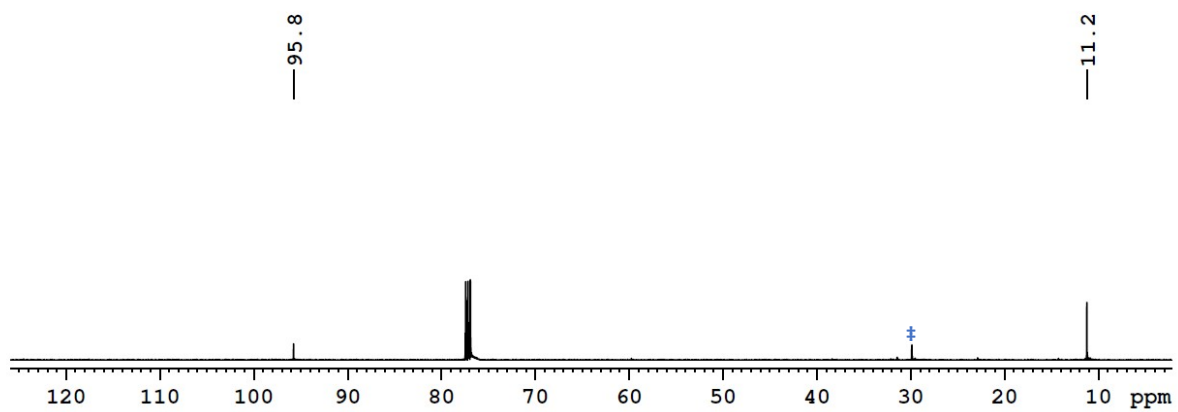


Figure S10. $^{13}\text{C}\{^1\text{H}\}$ NMR spectrum of **1** in CDCl_3 . (*H-Grease)

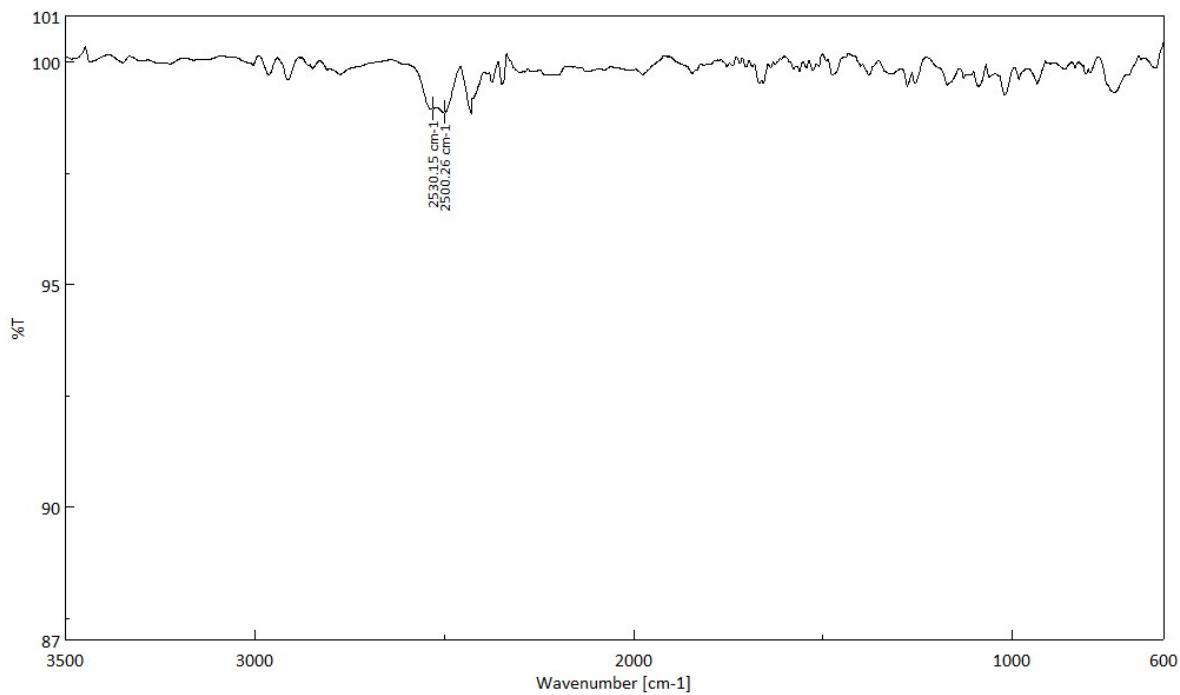


Figure S11. IR spectrum of **1** in CH₂Cl₂.

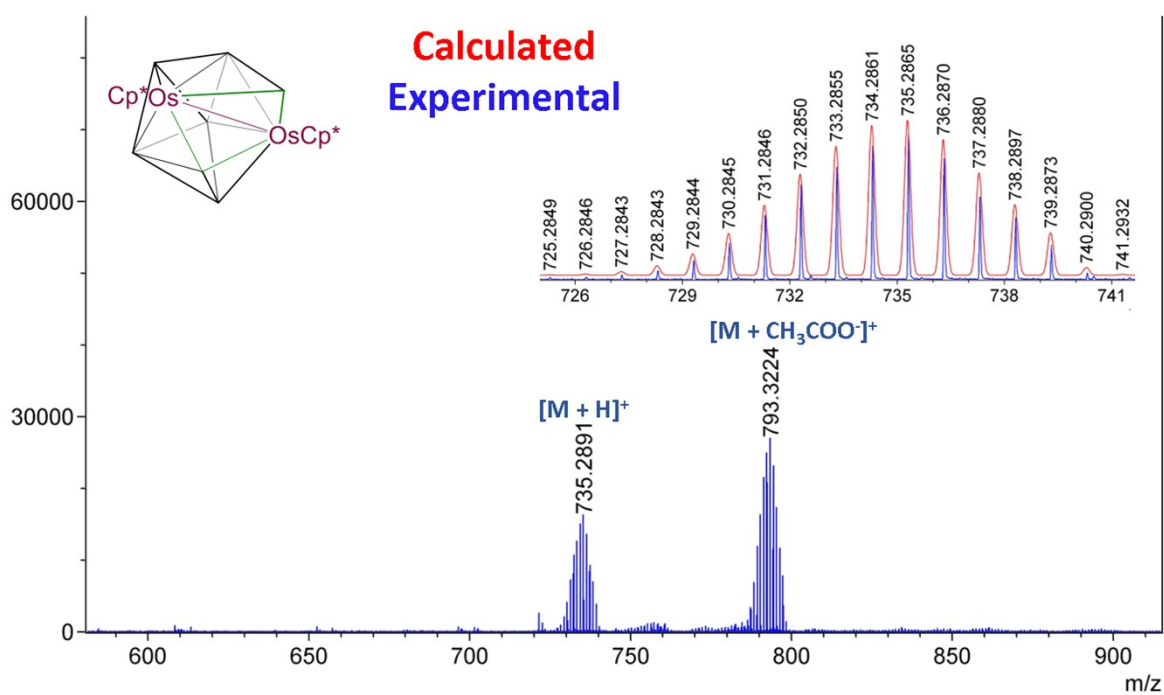


Figure S12. ESI-MS spectrum of **2**.

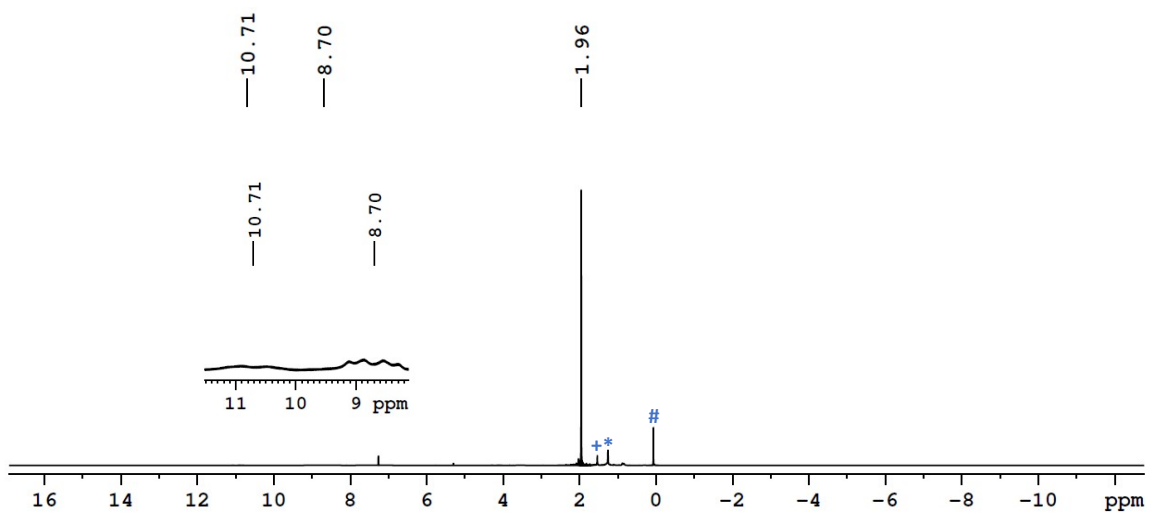


Figure S13. ^1H NMR spectrum of **2** in CDCl_3 . (#Silicon grease, + H_2O , *Hexane)

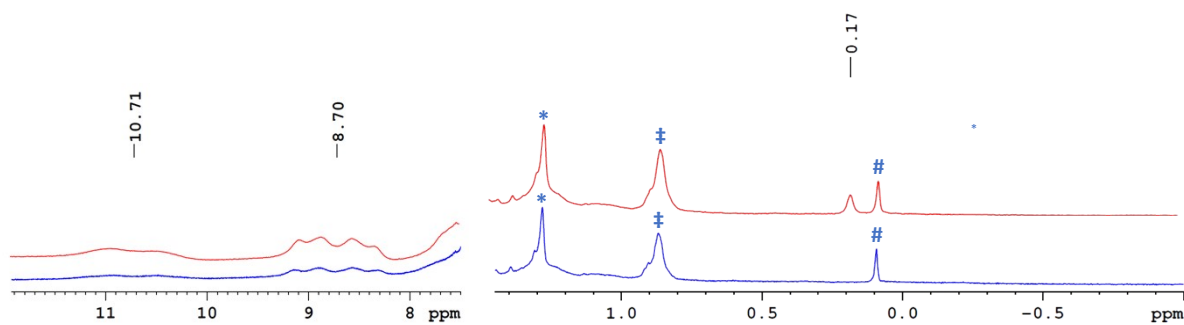


Figure S14. Stacked ^1H (blue) and $^1\text{H}\{^{11}\text{B}\}$ (red) NMR spectra of **2** in CDCl_3 . (#Silicon grease, +H-Grease, *Hexane)

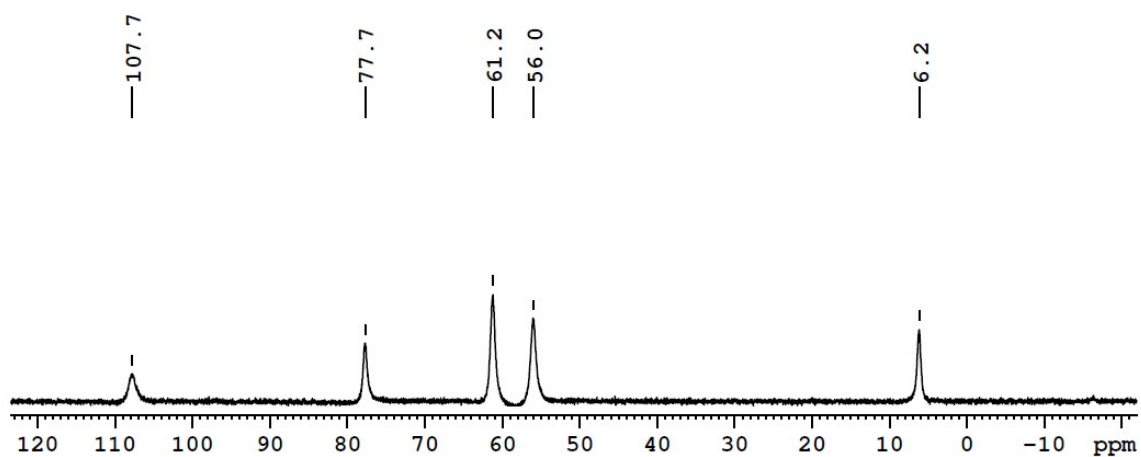


Figure S15. $^{11}\text{B}\{^1\text{H}\}$ NMR spectrum of **2** in CDCl_3 .

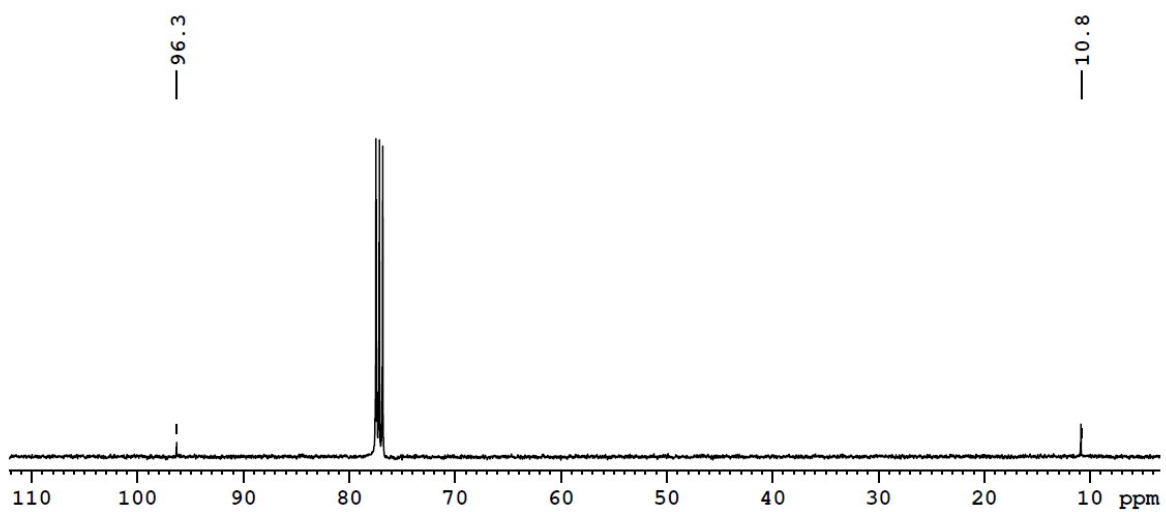


Figure S16. $^{13}\text{C}\{^1\text{H}\}$ NMR spectrum of **2** in CDCl_3 .

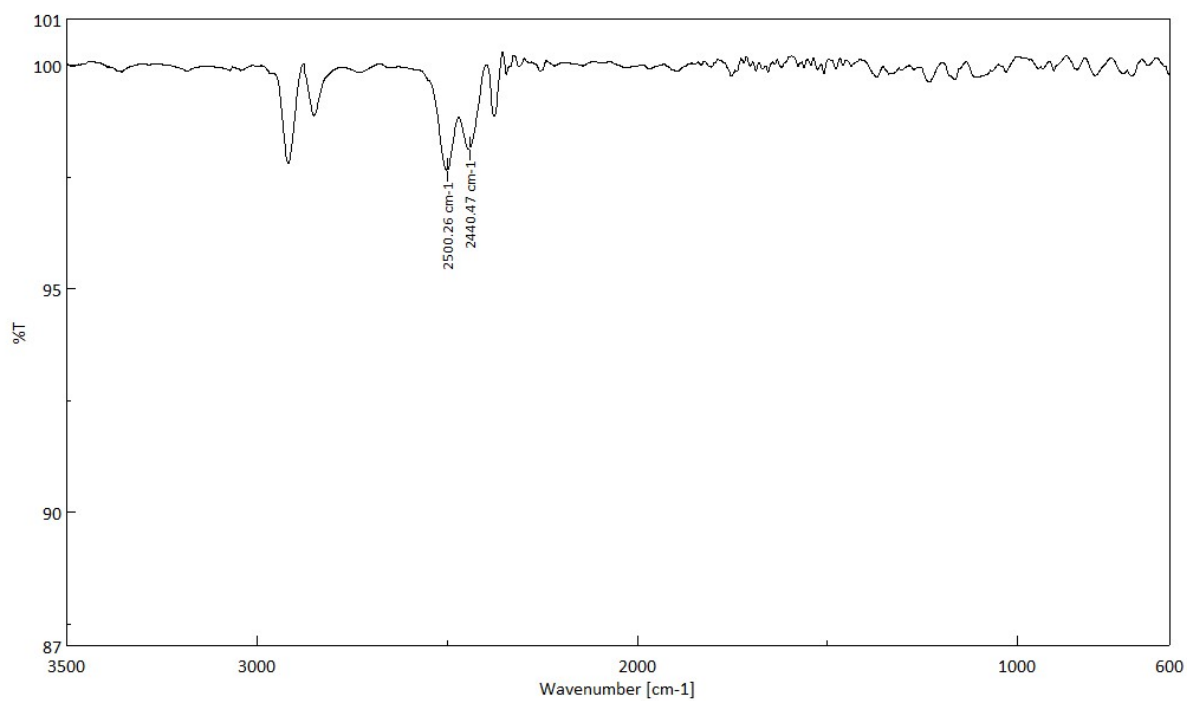


Figure S17. IR spectrum of **2** in CH_2Cl_2 .

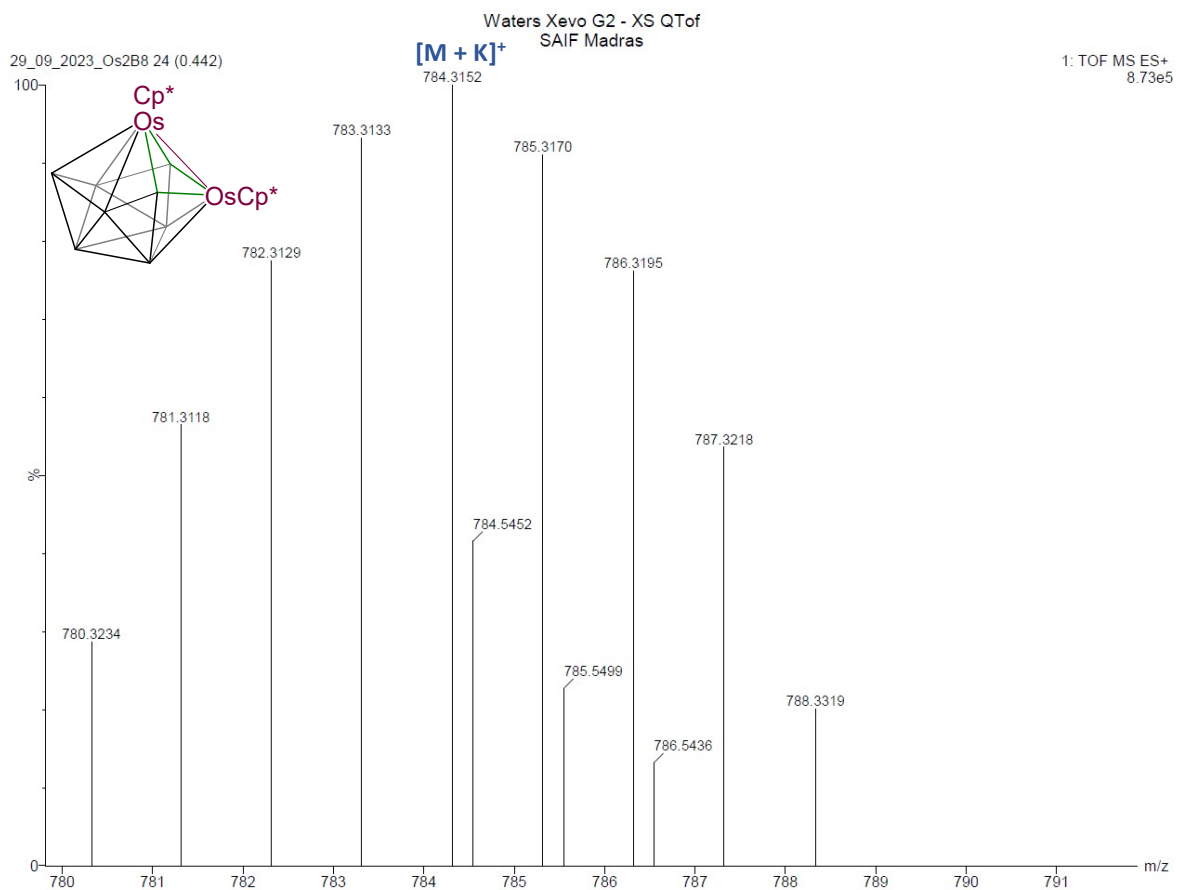


Figure S18. ESI-MS spectrum of 3.

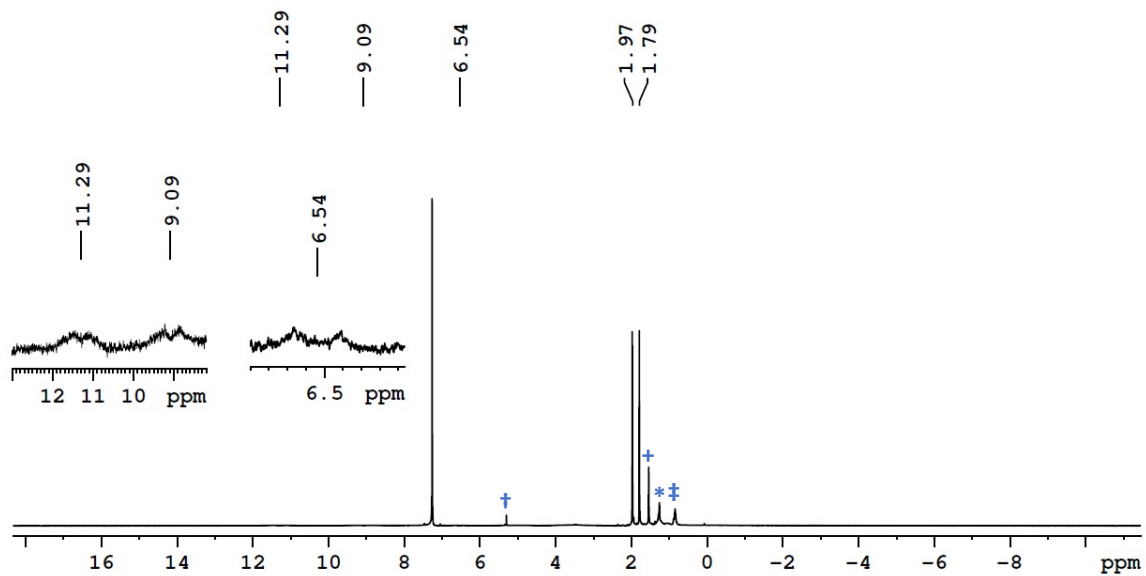


Figure S19. ¹H NMR spectrum of 3 in CDCl₃. (†H-Grease, †CH₂Cl₂, +H₂O, *Hexane)

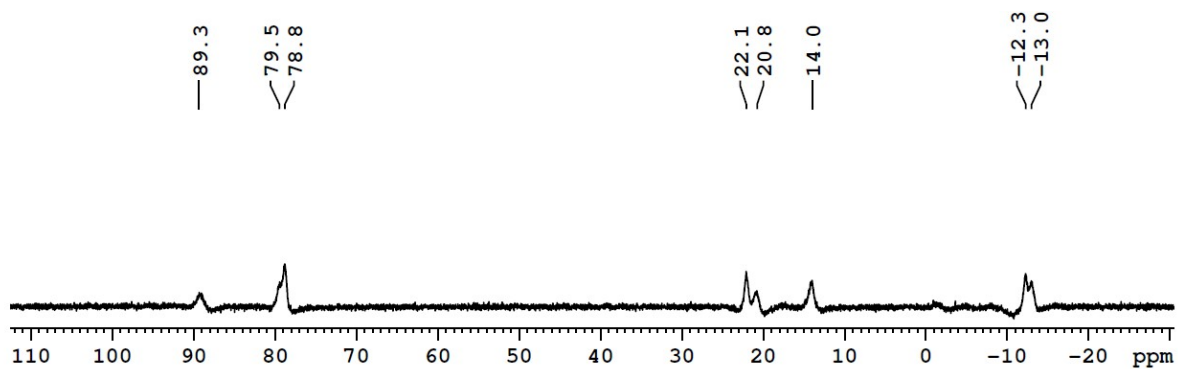


Figure S20. $^{11}\text{B}\{^1\text{H}\}$ NMR spectrum of **3** in CDCl_3 .

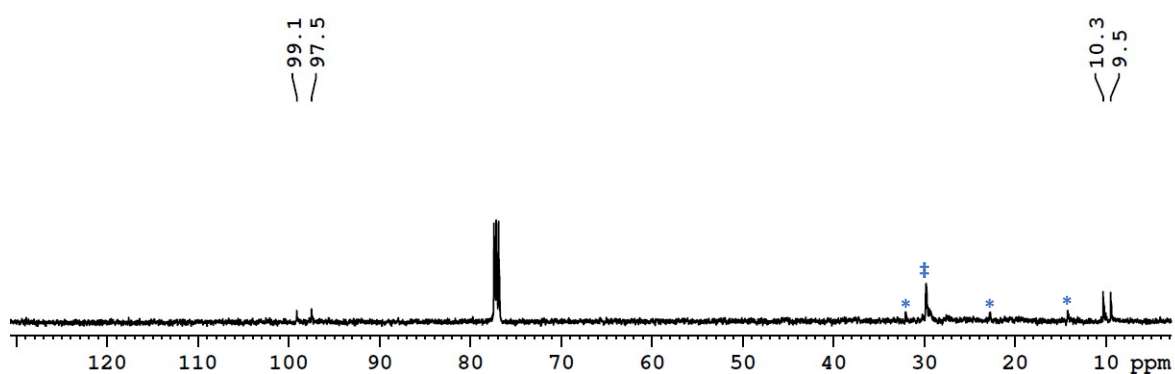


Figure S21. $^{13}\text{C}\{^1\text{H}\}$ NMR spectrum of **3** in CDCl_3 . (‡H-Grease, *Hexane).

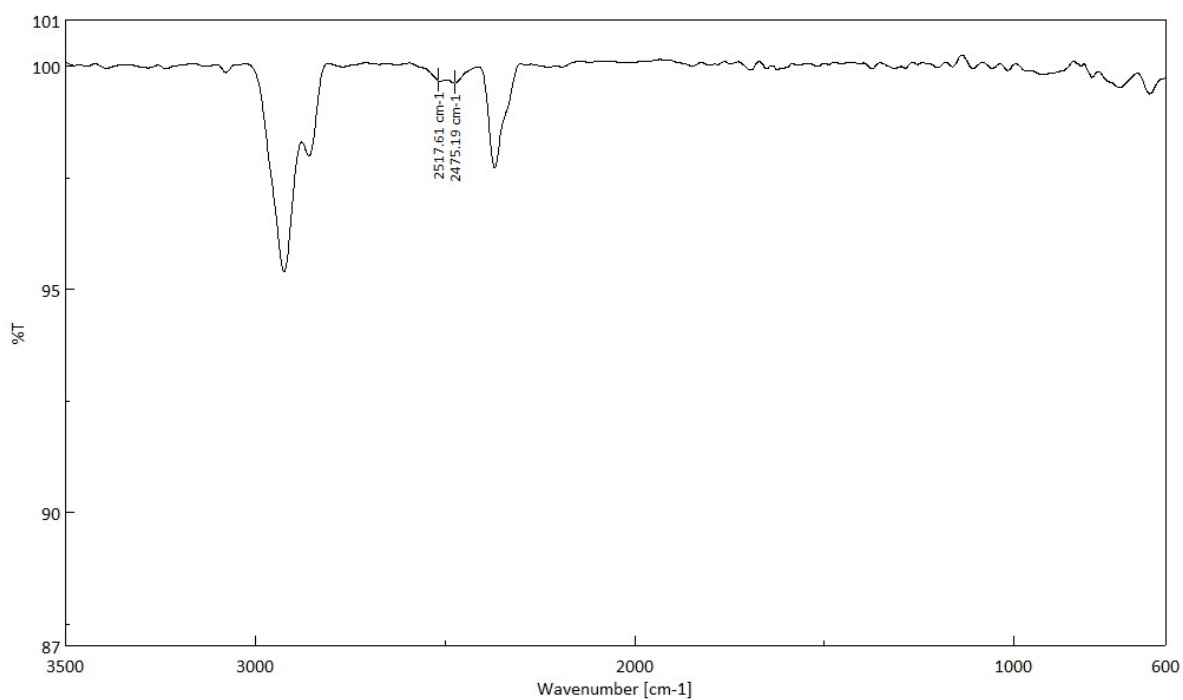


Figure S22. IR spectrum of **3** in CH_2Cl_2 .

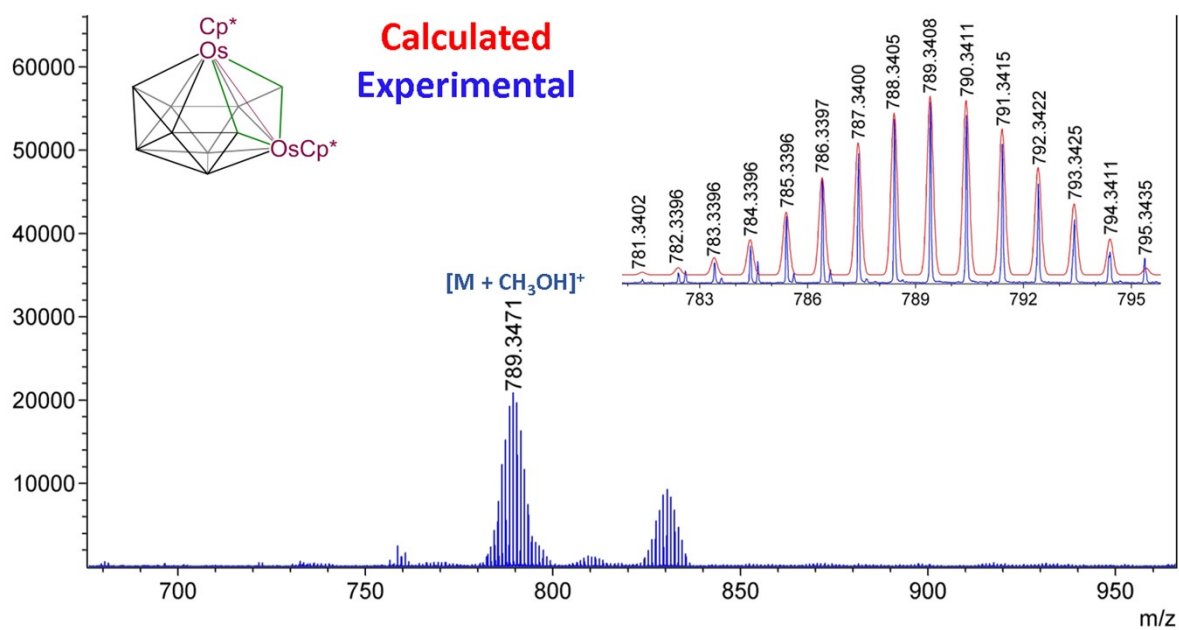


Figure S23. ESI-MS spectrum of **4**.

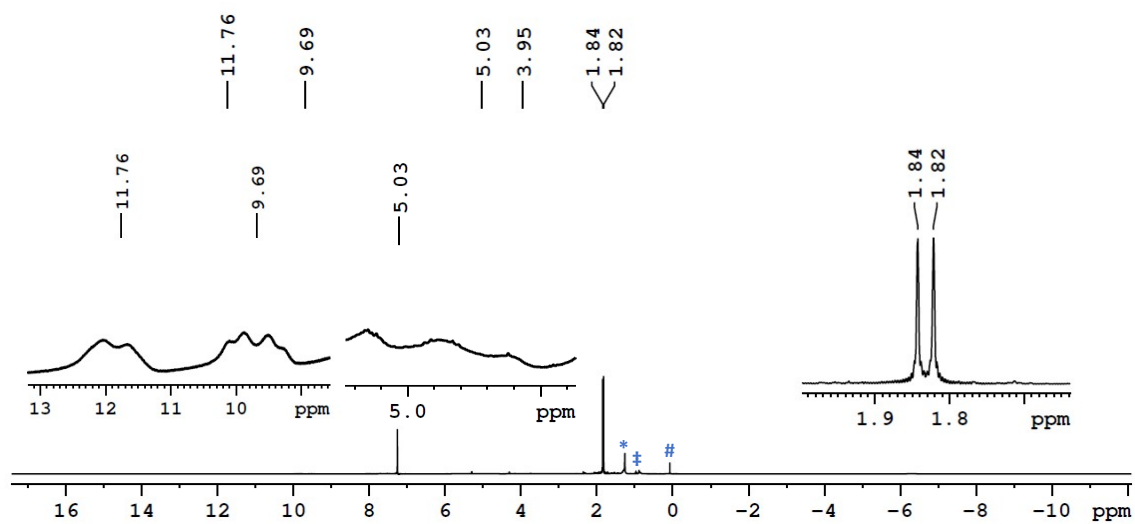


Figure S24. 1H NMR spectrum of **4** in $CDCl_3$. (# Silicon grease, ‡H-Grease, *Hexane).

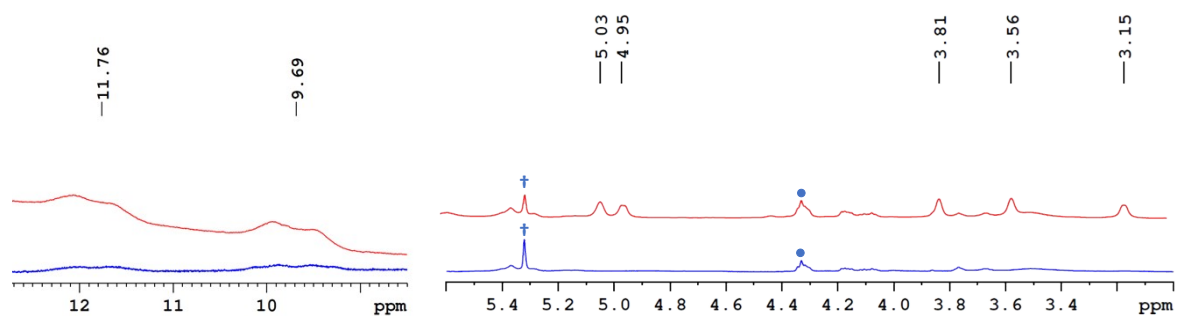


Figure S25. Stacked ^1H (blue) and $^1\text{H}\{^{11}\text{B}\}$ (red) NMR spectra of **4** in CDCl_3 . (+ CH_2Cl_2 , •Inseparable impurity).

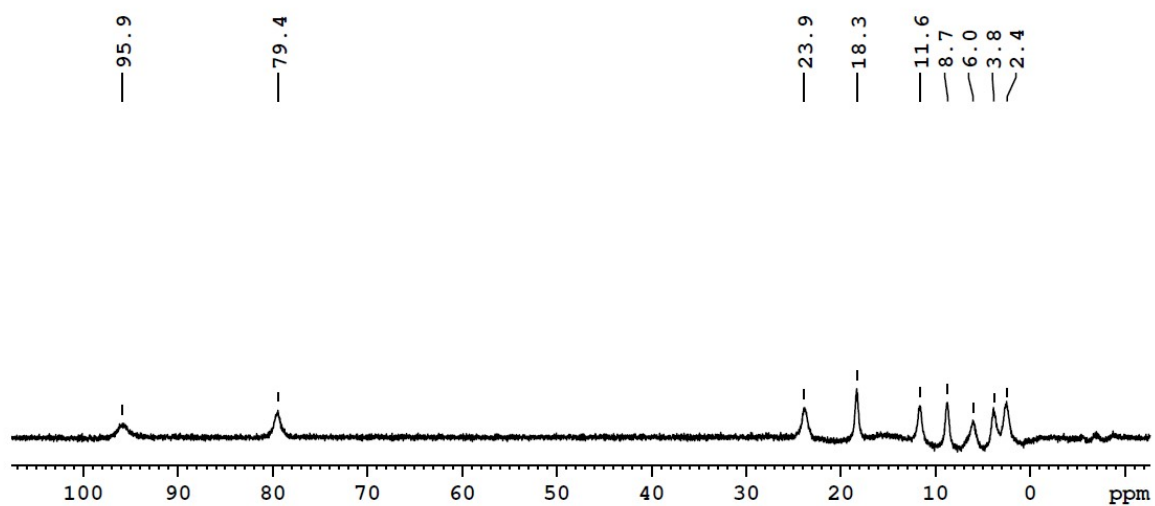


Figure S26. $^{11}\text{B}\{^1\text{H}\}$ NMR spectrum of **4** in CDCl_3 .

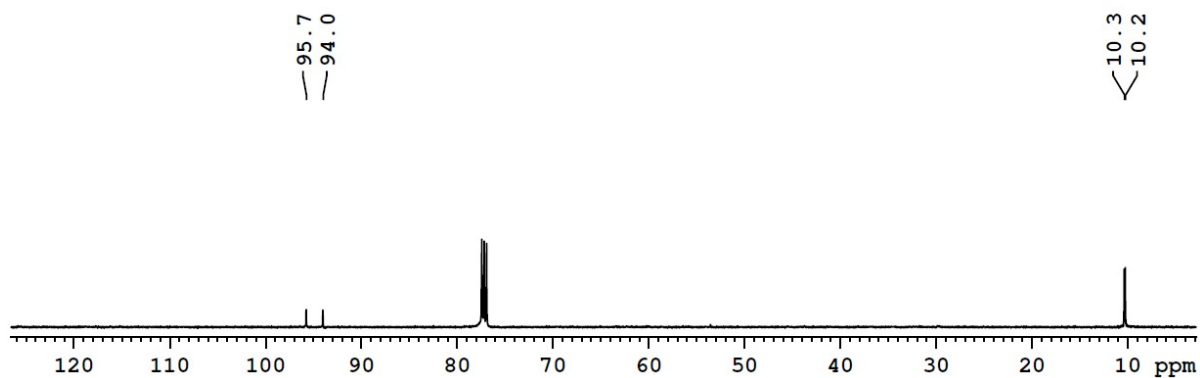


Figure S27. $^{13}\text{C}\{^1\text{H}\}$ NMR spectrum of **4** in CDCl_3 .

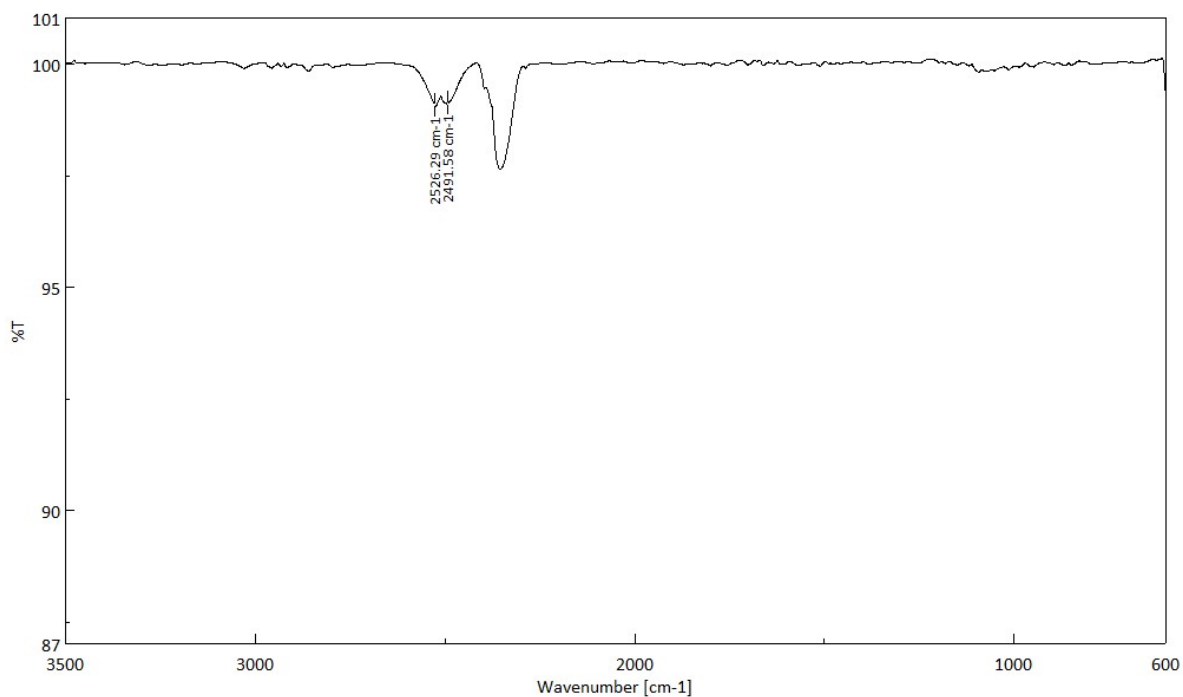


Figure S28. IR spectrum of 4 in CH₂Cl₂.

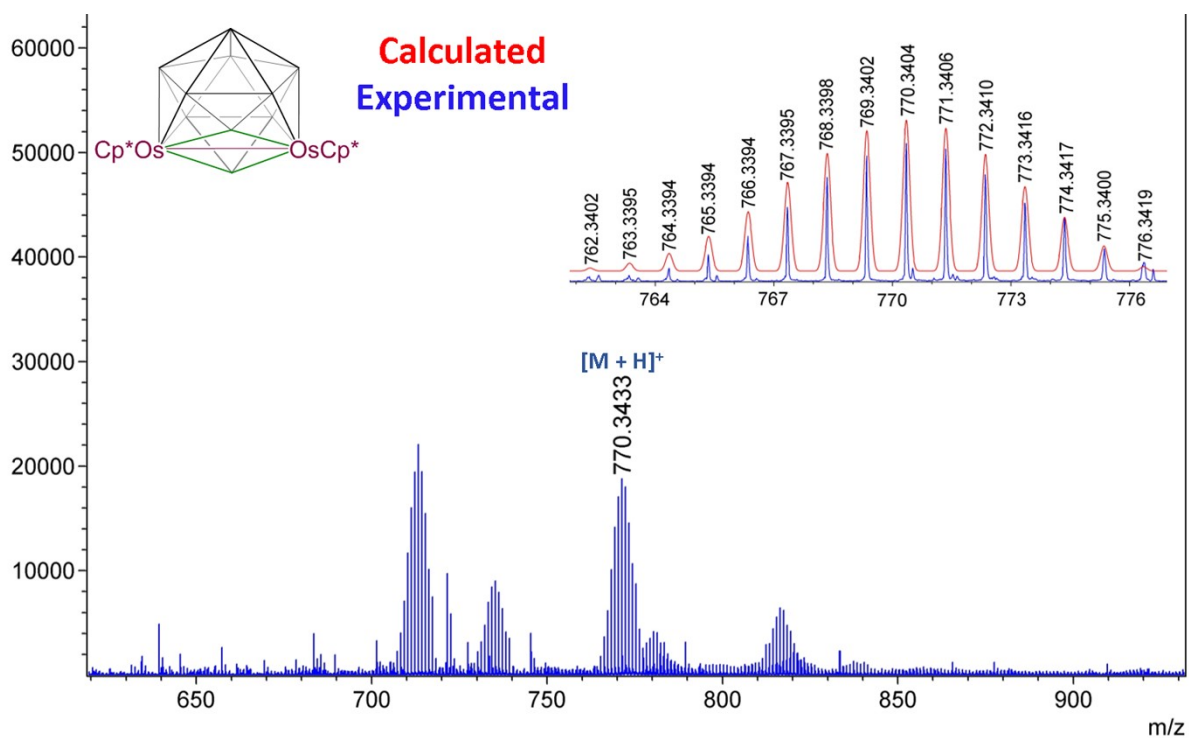


Figure 29. ESI-MS spectrum of 5.

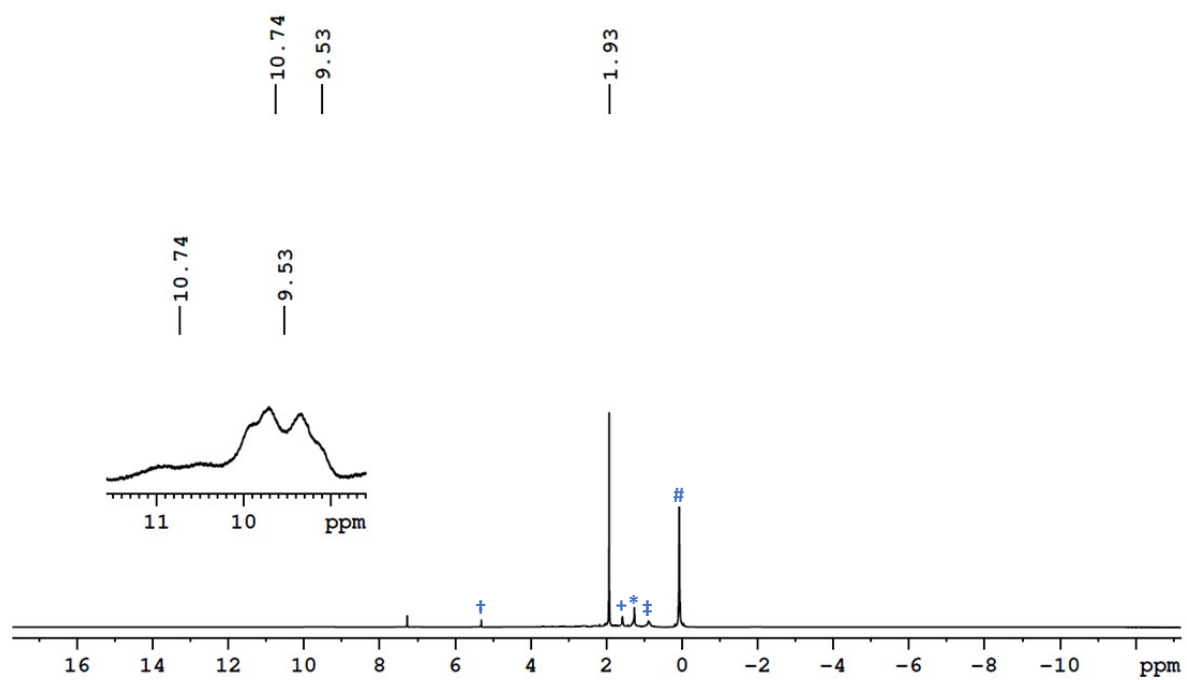


Figure S30. ^1H NMR spectrum of **5** in CDCl_3 . (#Silicon grease, ‡H-Grease, †CH₂Cl₂, †H₂O, *Hexane)

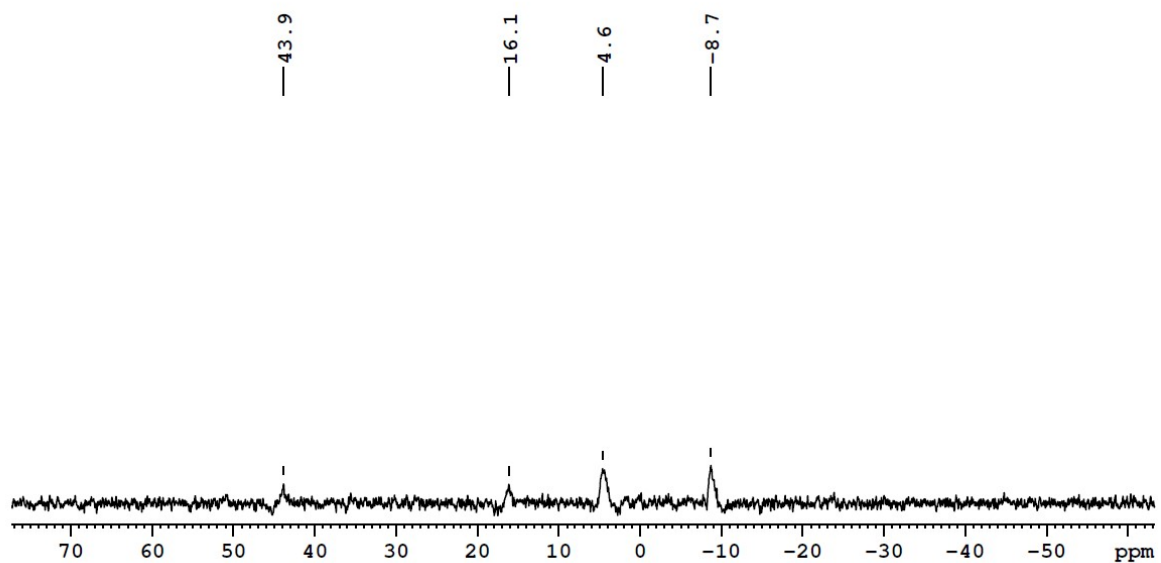


Figure S31. $^{11}\text{B}\{^1\text{H}\}$ NMR spectrum of **5** in CDCl_3 .

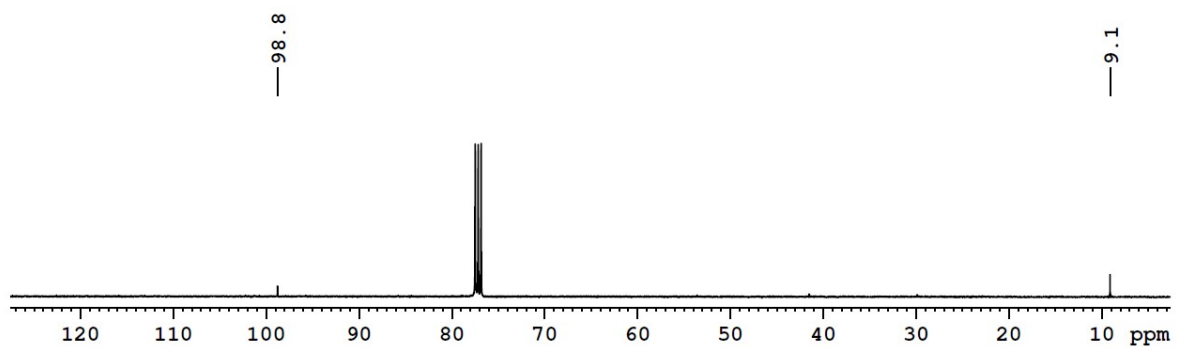


Figure S32. $^{13}\text{C}\{^1\text{H}\}$ NMR spectrum of **5** in CDCl_3 .

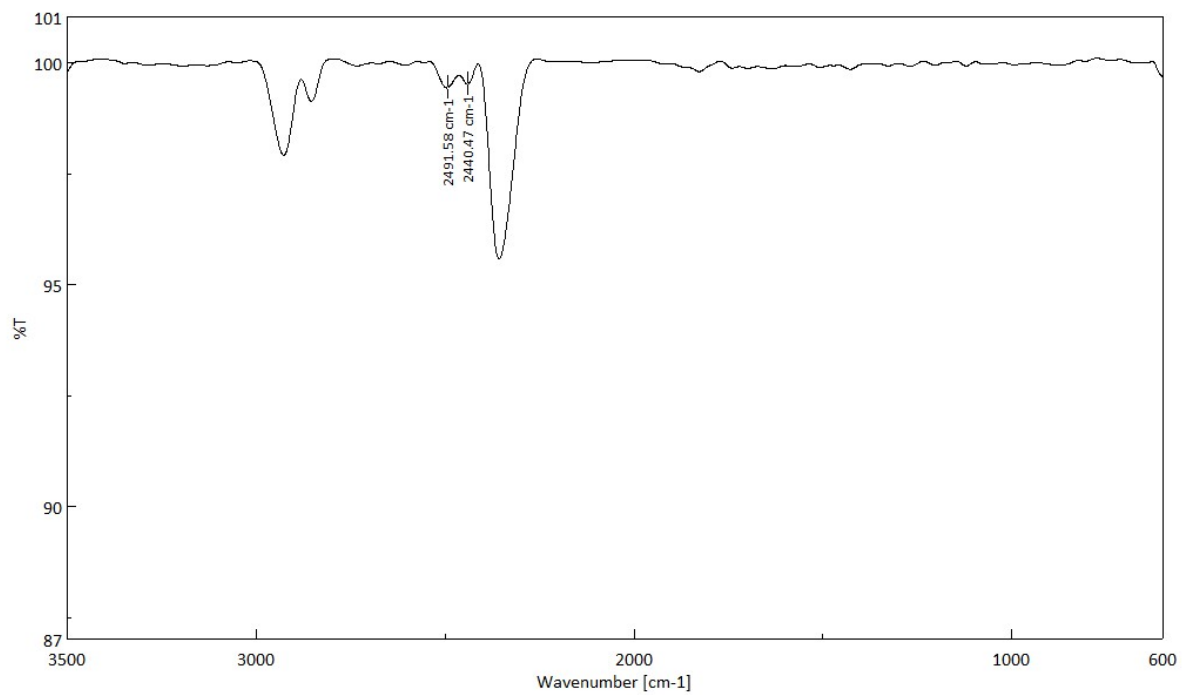


Figure S33. IR spectrum of **5** in CH_2Cl_2 .

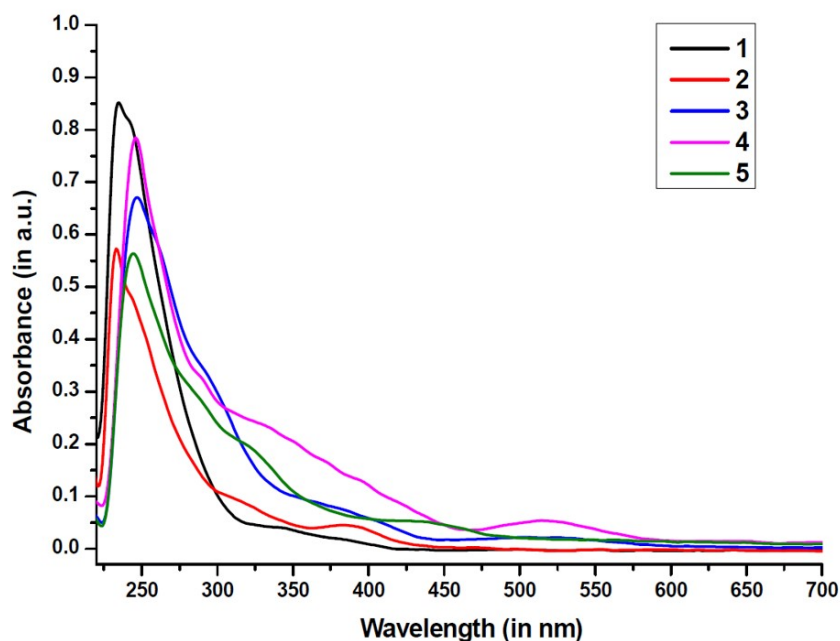


Figure S34. UV-Vis spectra of **1-5** in CH₂Cl₂.

I.3 X-ray Analysis Details

Suitable X-ray quality crystals of **1**, **2**, **3**, **4** and **5** were grown by slow diffusion of a hexane-CH₂Cl₂ solution at -4 °C. Crystal data of **1**, **3**, **4** and **5** were obtained and integrated using a D8 VENTURE Bruker AXS diffractometer with PHOTON II detector with graphite monochromated Mo-K α ($\lambda = 0.71073$ Å) radiation at 298(2) K for **1**, **4**, **5** and for **3** 297(2) K. Crystal data of **2** was obtained and integrated using a Bruker APEX-II CCD diffractometer with graphite monochromated Mo-K α ($\lambda = 0.71073$ Å) radiation at 296(2) K. All the structures were solved using SHELXT-2018 and SHELXS-97³ and refined using SHELXL-2018, SHELXL-2014 and SHELXL-2019⁴. Using Olex2 all the molecular structures were drawn.⁵ Crystallographic data have been deposited with the Cambridge Crystallographic Data Center as supplementary publication no CCDC- 2291109 (**1**), 2293942 (**2**), 2300469 (**3**), 2291111 (**4**) and 2291112 (**5**). These data can be obtained free of charge from The Cambridge Crystallographic Data Centre via www.ccdc.cam.ac.uk/data_request/cif.

Crystal data for **1**: C₂₀H₃₆B₆Os₂, $M_r = 721.75$, Monoclinic, space group $P 21/c$, $a = 8.5352(2)$ Å, $b = 14.7848(4)$ Å, $c = 20.0361(6)$ Å, $\alpha = 90^\circ$, $\beta = 101.894(1)^\circ$, $\gamma = 90^\circ$, $V = 2474.10(12)$ Å³, $Z = 4$, $\rho_{\text{calcd}} = 1.938$ g/cm³, $\mu = 10.265$ mm⁻¹, $F(000) = 1352.0$, $R_1 = 0.0304$, $wR_2 = 0.0588$, 6944 independent reflections [$2\theta \leq 59.154^\circ$] and 260 parameters.

Crystal data for **2**: $C_{20}H_{37}B_7Os_2$, $M_r = 733.56$, Tetragonal, space group $P -4 21 c$, $a = 23.6454(8)$ Å, $b = 23.6454(8)$ Å, $c = 8.8984(3)$ Å, $\alpha = 90^\circ$, $\beta = 90^\circ$, $\gamma = 90^\circ$, $V = 4975.1(4)$ Å³, $Z = 8$, $\rho_{\text{calcd}} = 1.959$ g/cm³, $\mu = 10.211$ mm⁻¹, $F(000) = 2752.0$, $R_1 = 0.0218$, $wR_2 = 0.0376$, 4381 independent reflections [$2\theta \leq 49.974^\circ$] and 272 parameters.

Crystal data for **3**: $C_{20}H_{38}B_8Os_2$, $M_r = 745.38$, Monoclinic, space group $C c$, $a = 9.172(3)$ Å, $b = 15.337(5)$ Å, $c = 19.588(6)$ Å, $\alpha = 90^\circ$, $\beta = 103.464(10)^\circ$, $\gamma = 90^\circ$, $V = 2679.6(14)$ Å³, $Z = 4$, $\rho_{\text{calcd}} = 1.848$ g/cm³, $\mu = 9.480$ mm⁻¹, $F(000) = 1400.0$, $R_1 = 0.0343$, $wR_2 = 0.0740$, 5967 independent reflections [$2\theta \leq 56.64^\circ$] and 345 parameters.

Crystal data for **4**: $C_{20}H_{39}B_9Os_2$, $M_r = 757.20$, Monoclinic, space group $P 21/n$, $a = 8.9252(10)$ Å, $b = 14.6904(16)$ Å, $c = 20.153(2)$ Å, $\alpha = 90^\circ$, $\beta = 99.649(5)^\circ$, $\gamma = 90^\circ$, $V = 2605.0(5)$ Å³, $Z = 4$, $\rho_{\text{calcd}} = 1.931$ g/cm³, $\mu = 9.753$ mm⁻¹, $F(000) = 1424.0$, $R_1 = 0.0489$, $wR_2 = 0.1139$, 4586 independent reflections [$2\theta \leq 49.998^\circ$] and 284 parameters.

Crystal data for **5**: $C_{20}H_{40}B_{10}Os_2$, $M_r = 769.02$, Monoclinic, space group $P 21/n$, $a = 8.891(8)$ Å, $b = 15.195(11)$ Å, $c = 19.952(18)$ Å, $\alpha = 90^\circ$, $\beta = 100.42(3)^\circ$, $\gamma = 90^\circ$, $V = 2651(4)$ Å³, $Z = 4$, $\rho_{\text{calcd}} = 1.927$ g/cm³, $\mu = 9.584$ mm⁻¹, $F(000) = 1448.0$, $R_1 = 0.0910$, $wR_2 = 0.2329$, 4642 independent reflections [$2\theta \leq 49.996^\circ$] and 250 parameters.

II Computational Details

All molecules were fully optimized using the *Gaussian 09*⁶ program employing the bp86 functional⁷ in conjunction with a def2-svp basis set from EMSL Basis Set Exchange Library.⁸ The model compounds were fully optimized in gaseous state (no solvent effect) starting from the X-ray crystallographic coordinates. The calculations were performed with the Cp analogues instead of Cp* to save computing time. Frequency calculations were performed at the same level of theory to verify the nature of the stationary states and the absence of any imaginary frequency to confirm that all structures represent minima on the potential energy hypersurface. Natural bonding analyses were performed with the natural bond orbital (NBO) partitioning scheme⁹ as implemented in the Gaussian 09 suite of programs. Wiberg bond indexes (WBI)¹⁰ were obtained from a natural bond orbital analysis. All the optimized structures and orbital graphics were generated using the Gaussview¹¹, and Chemcraft¹² visualization programs.

Table S1. Bond parameters of clusters **1-5** are compared with their optimized values and WBIs. All distances are in Å. Θ are the dihedral angles.

[(Cp*Os) ₂ B ₆ H ₆] (1)				[(Cp*Os) ₂ B ₇ H ₇] (2)			
	Expt.	Cal.	WBI		Expt.	Cal.	WBI
Os1-Os2	2.7688(3)	2.7577	0.367	Os1-Os2	2.8051(5)	2.8492	0.371
Os1-B4	2.055(8)	2.088	0.683	Os1-B1	2.081(12)	2.109	0.651
Os1-B5	2.060(7)	2.088	0.683	Os1-B4	2.236(14)	2.276	0.401
Os1-B1	2.134(8)	2.152	0.557	Os1-B5	2.030(11)	2.066	0.712
Os1-B2	2.249(9)	2.265	0.404	Os1-B6	2.091(13)	2.097	0.625
Os1-B6	2.303(12)	2.265	0.404	Os1-B7	2.246(13)	2.335	0.369
Os2-B4	2.062(7)	2.088	0.683	Os2-B1	2.180(11)	2.239	0.498
Os2-B5	2.084(8)	2.088	0.683	Os2-B2	2.121(15)	2.125	0.583
Os2-B3	2.155(8)	2.152	0.557	Os2-B3	2.222(12)	2.308	0.407
Os2-B6	2.234(11)	2.265	0.404	Os2-B4	2.179(13)	2.205	0.456
Os2-B2	2.298(12)	2.265	0.404	Os2-B5	2.040(12)	2.097	0.656
B1-B6	1.735(14)	1.757	0.603	B1-B2	1.72(2)	1.778	0.538
B1-B3	1.742(13)	1.745	0.611	B1-B7	1.84(2)	1.818	0.542
B1-B2	1.759(14)	1.757	0.603	B2-B7	1.66(2)	1.706	0.682
B2-B3	1.699(14)	1.757	0.602	B2-B3	1.71(2)	1.802	0.503
B2-B5	1.765(14)	1.807	0.539	B3-B6	1.73(2)	1.791	0.555
B3-B6	1.691(14)	1.757	0.603	B3-B4	1.76(2)	1.752	0.621
B4-B6	1.755(14)	1.807	0.539	B3-B7	1.98(2)	1.939	0.432
Θ (B4-Os1-Os2-B5)	145.33°	140.13°	-	B4-B6	1.67(2)	1.774	0.547
				B4-B5	1.78(2)	1.803	0.530
				B6-B7	1.71(2)	1.783	0.537
				Θ (B1-Os1-Os2-B5)	152.17°	152.50°	-
[(Cp*Os) ₂ B ₈ H ₈] (3)				[(Cp*Os) ₂ B ₉ H ₉] (4)			
	Expt.	Cal.	WBI		Expt.	Cal.	WBI
Os1-Os2	2.9046(11)	2.6300	0.756	Os1-Os2	2.8505(7)	2.8580	0.351
Os1-B5	2.14(4)	2.250	0.421	Os1-B1	2.293(19)	2.431	0.326
Os1-B6	2.18(4)	2.242	0.411	Os1-B2	2.229(18)	2.208	0.482
Os1-B7	2.22(4)	2.118	0.600	Os1-B3	2.321(18)	2.382	0.343
Os1-B8	2.13(3)	2.105	0.594	Os1-B7	2.159(17)	2.226	0.489
Os2-B1	2.28(4)	2.111	0.590	Os1-B8	2.210(19)	2.259	0.368
Os2-B3	2.35(3)	2.358	0.330	Os1-B9	2.175(17)	2.252	0.473
Os2-B4	2.48(5)	2.366	0.331	Os2-B4	2.217(18)	2.257	0.406
Os2-B7	2.16(3)	2.166	0.550	Os2-B5	2.212(19)	2.270	0.413
Os2-B8	2.14(3)	2.204	0.507	Os2-B7	2.138(17)	2.115	0.599
B1-B4	1.68(6)	1.760	0.577	Os2-B8	2.13(2)	2.135	0.474
B1-B2	1.77(5)	1.742	0.570	Os2-B9	2.051(18)	2.121	0.612
B1-B3	1.78(5)	1.754	0.586	B1-B2	1.49(4)	1.735	0.603
B2-B4	1.77(6)	1.838	0.479	B1-B6	1.70(4)	1.829	0.491
B2-B6	1.78(5)	1.821	0.505	B1-B8	1.77(3)	1.679	0.684
B2-B5	1.78(5)	1.803	0.513	B1-B5	2.05(3)	1.907	0.420
B2-B3	1.80(5)	1.826	0.489	B2-B3	1.57(4)	1.722	0.626
B3-B5	1.79(5)	1.778	0.573	B2-B6	1.82(3)	1.738	0.589
B3-B7	1.86(5)	1.783	0.585	B3-B7	1.69(3)	1.758	0.595
B4-B8	1.73(6)	1.745	0.627	B3-B4	1.70(3)	1.787	0.544
B4-B6	1.80(5)	1.792	0.548	B3-B6	1.85(4)	1.807	0.492
B5-B6	1.80(5)	1.902	0.470	B4-B6	1.73(3)	1.809	0.508
B5-B7	1.92(5)	1.874	0.472	B4-B7	1.83(3)	1.833	0.488
B6-B8	1.80(5)	1.827	0.526	B4-B5	1.86(4)	1.814	0.532
Θ (B7-Os1-Os2-B8)	152.11°	152.16°	-	B5-B6	1.74(4)	1.827	0.508
				B5-B8	1.91(3)	1.740	0.569
				B8-B9	1.52(3)	1.655	0.698
				Θ (B7-Os1-Os2-B9)	156.61°	157.30°	-

[(Cp*Os) ₂ B ₁₀ H ₁₀] (5)			
	Expt.	Cal.	WBI
Os1-Os2	2.832(2)	2.591	0.836
Os1-B1	2.14(4)	2.151	0.520
Os1-B2	2.20(4)	2.309	0.346
Os1-B3	2.22(4)	2.237	0.453
Os1-B8	2.57(4)	2.309	0.346
Os1-B9	2.19(4)	2.151	0.520
Os2-B1	2.15(4)	2.151	0.520
Os2-B5	2.20(4)	2.238	0.453
Os2-B6	2.24(4)	2.309	0.346
Os2-B9	2.16(4)	2.151	0.520
Os2-B10	2.19(4)	2.309	0.346
B1-B6	1.69(5)	1.766	0.579
B1-B2	1.79(5)	1.766	0.579
B2-B3	1.76(6)	1.839	0.506
B2-B7	1.77(6)	1.782	0.526
B2-B6	1.79(6)	1.790	0.521
B3-B4	1.65(5)	1.801	0.497
B3-B7	1.73(6)	1.801	0.497
B3-B8	1.97(6)	1.839	0.506
B4-B8	1.64(5)	1.782	0.526
B4-B5	1.67(6)	1.801	0.497
B4-B7	1.73(6)	1.798	0.519
B4-B10	1.77(6)	1.782	0.527
B5-B7	1.67(6)	1.801	0.497
B5-B10	1.77(6)	1.840	0.505
B5-B6	1.83(6)	1.840	0.505
B6-B7	1.71(6)	1.782	0.527
B8-B10	1.58(5)	1.789	0.521
B8-B9	1.71(5)	1.766	0.579
B9-B10	1.59(5)	1.766	0.579
∠ (B1-Os1-Os2-B9)	176.39°	176.40°	-

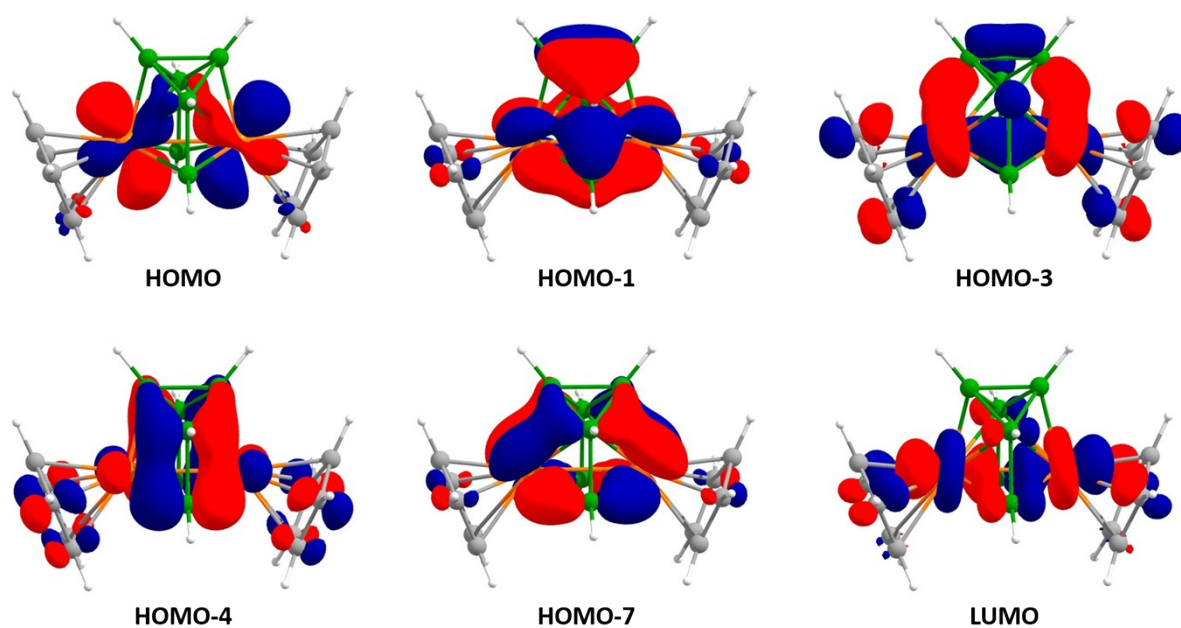


Figure S35. Selected molecular orbitals of cluster **1** (isocontour values: ± 0.043 [e.bohr⁻³]^{1/2}).

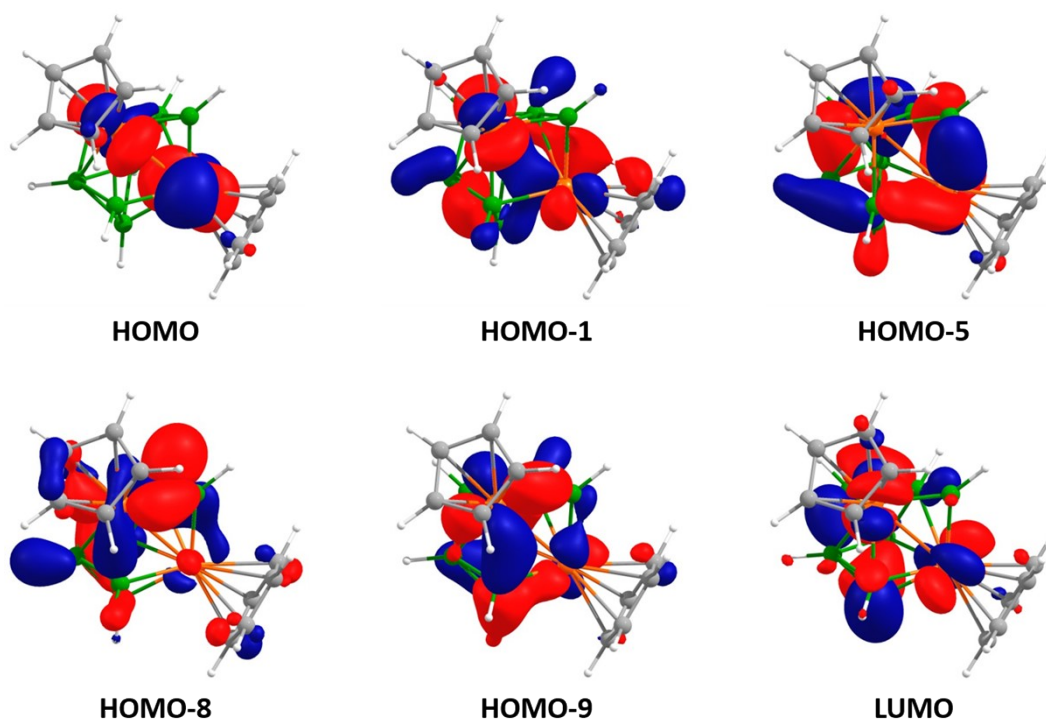


Figure S36. Selected molecular orbitals of cluster **2** (isocontour values: ± 0.043 [e.bohr⁻³]^{1/2}).

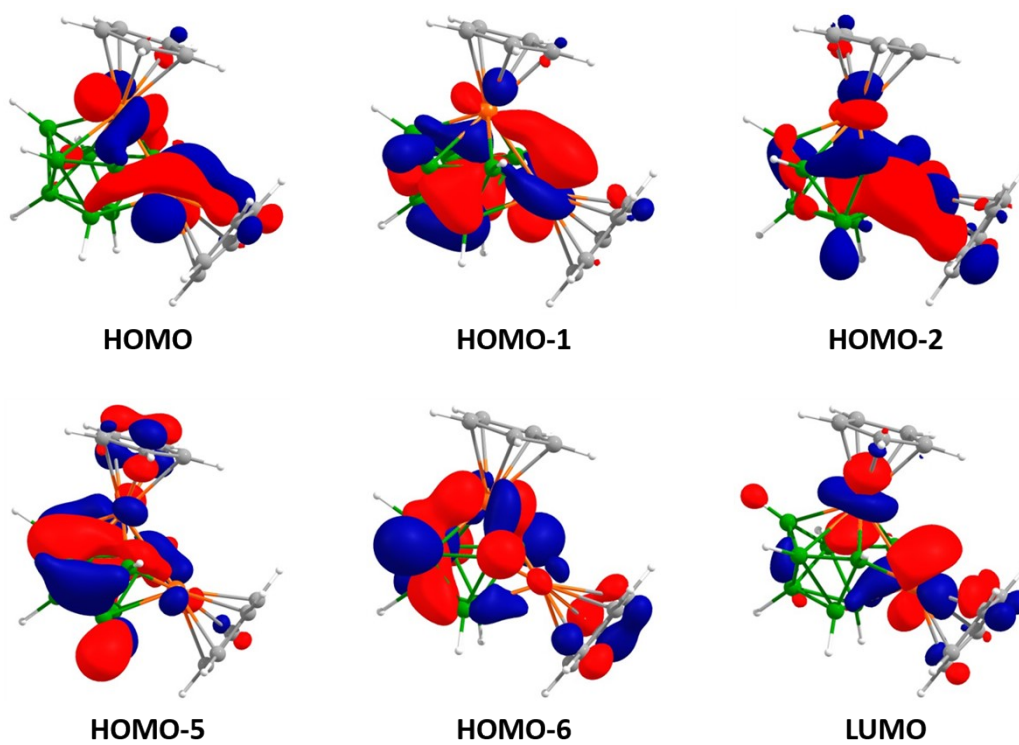


Figure S37. Selected molecular orbitals of cluster **3** (isocontour values: ± 0.043 [e.bohr⁻³]^{1/2}).

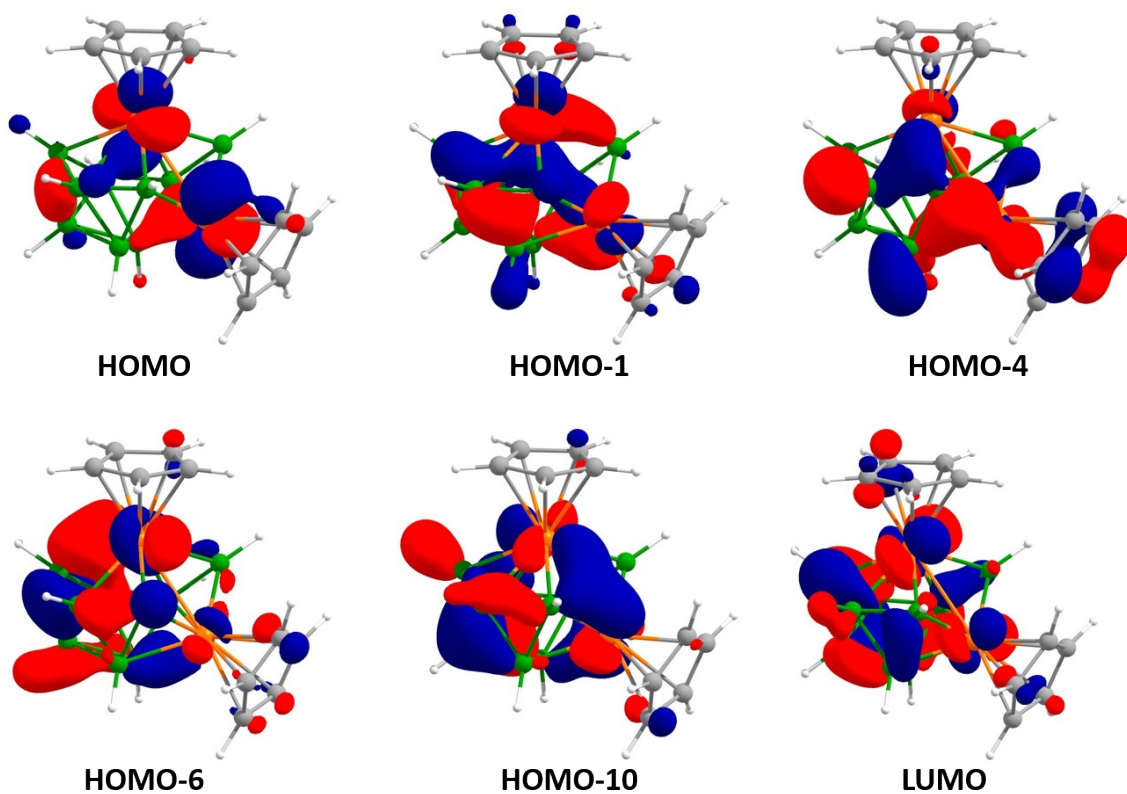


Figure S38. Selected molecular orbitals of cluster 4 (isocontour values: ± 0.043 [e.bohr⁻³]^{1/2}).

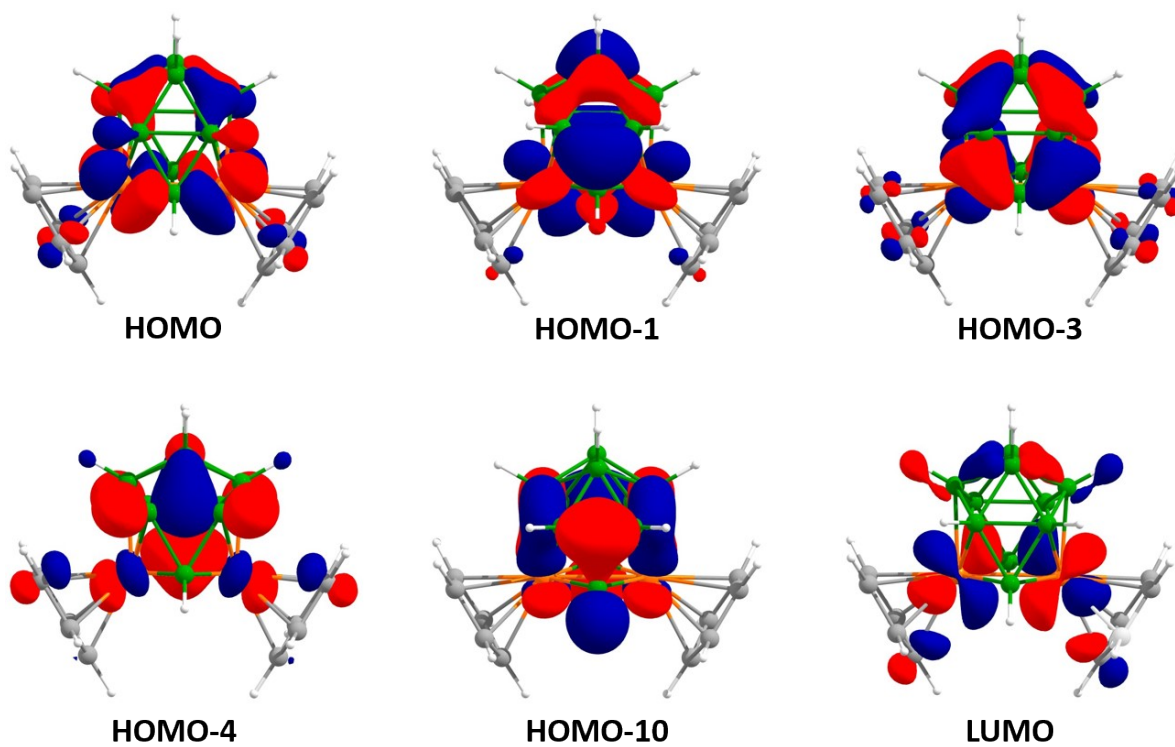


Figure S39. Selected molecular orbitals of cluster 5 (isocontour values: ± 0.043 [e.bohr⁻³]^{1/2}).

Table S2. Calculated natural charges (q_{Os} , and q_B), natural valence populations (Pop) and HOMO–LUMO gaps (ΔE_{H-L}) of clusters **1-5**.

Compounds	q_{Os}	q_B	$Pop (Os_{val})$	$Pop (B_{val})$	ΔE_{H-L} (eV)
1	-0.493	0.005	8.490	2.964	3.333
	-0.493	-0.148	8.490	3.115	
		0.005		2.964	
		0.362		2.602	
		-0.148		3.115	
		0.362		2.602	
2	-0.437	0.110	8.437	2.850	2.031
	-0.421	0.001	8.415	2.961	
		-0.062		3.028	
		-0.157		3.122	
		0.344		2.620	
		0.074		2.892	
		-0.118		3.085	
3	-0.225	-0.013	8.230	2.976	0.518
	-0.289	-0.118	8.287	3.087	
		-0.158		3.125	
		-0.154		3.121	
		-0.038		3.001	
		-0.050		3.015	
		0.112		2.846	
		0.038		2.921	
4	-0.405	-0.095	8.399	3.066	2.325
	-0.431	0.001	8.430	2.961	
		-0.185		3.151	
		-0.089		3.050	
		-0.038		3.005	
		-0.108		3.078	
		0.142		2.817	
		-0.132		3.093	
		0.213		2.754	
5	-0.243	0.027	8.246	2.930	0.851
	-0.242	-0.094	8.245	3.055	
		-0.063		3.027	
		-0.161		3.128	
		-0.062		3.025	
		-0.094		3.055	
		-0.161		3.128	
		-0.094		3.055	
		0.027		2.930	
		-0.094		3.055	

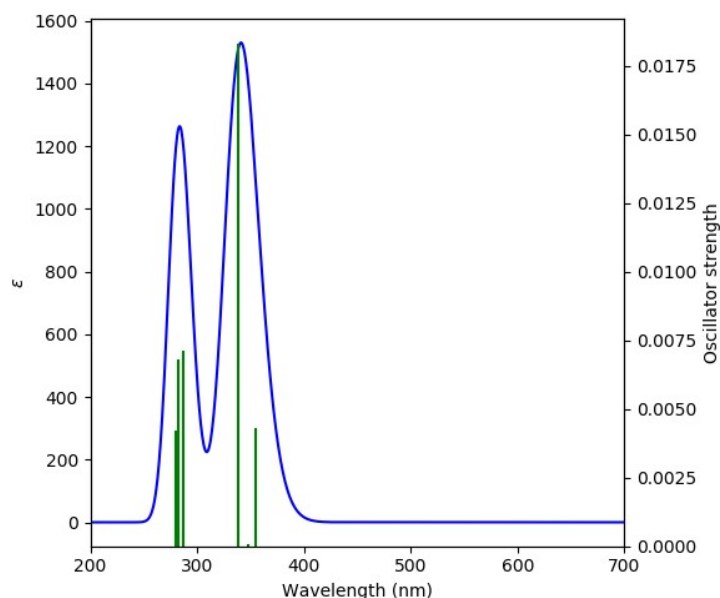


Fig. S40. Calculated absorption spectrum of **1** using TD-BP86/def2-svp level of theory.

Table S3. TD-DFT calculated electronic transition configuration for **1** along with their corresponding excitation energies, wavelength and oscillator strengths

HOMO is 69

No	Transition configurations (%) ^[a]	Excitation Energy (ev)	Wavelength (nm)		Osc, Strength
			Cal.	Expt.	
1	HOMO→LUMO(99)	3.4949	354.7574		0.0043
2	HOMO→LUMO+2(99)	3.5696	347.3335		0.0001
3	HOMO→LUMO+1(92)	3.6574	338.9954	342 ^[b]	0.0183
4	HOMO→LUMO+3(99)	3.9244	315.9315		0.0
5	HOMO-1→LUMO(95)	4.2594	291.0837		0.0
6	HOMO-3→LUMO(85)	4.3191	287.0602		0.0071
	HOMO-1→LUMO+2(11)				
7	HOMO-3→LUMO+2(86)	4.3810	283.0043		0.0
	HOMO-2→LUMO+2(13)				
8	HOMO-4→LUMO(40)	4.3896	282.4498		0.0068
	HOMO-1→LUMO+1(59)				
9	HOMO-3→LUMO+2(13)	4.3983	281.8911		0.0
	HOMO-2→LUMO+2(83)				
10	HOMO-3→LUMO(12)	4.4266	280.0889		0.0042
	HOMO-2→LUMO(30)				
	HOMO-2→LUMO+2(32)				
	HOMO→LUMO+4(24)				

^[a]components with greater than 10% contribution shown, ^[b]shoulder peak

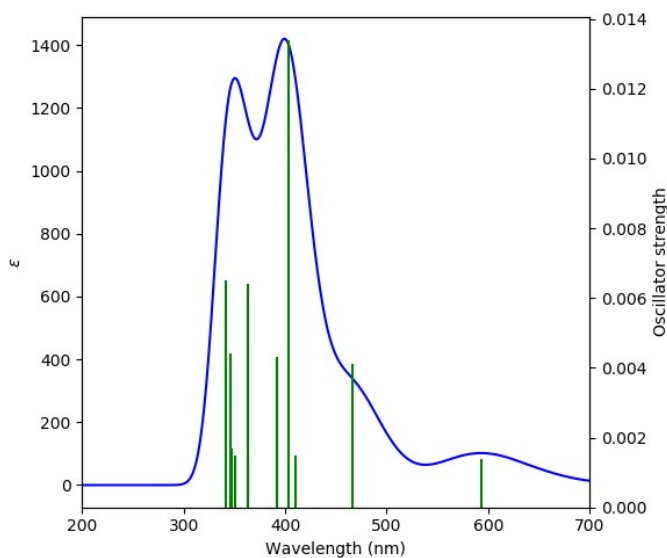


Fig. S41. Calculated absorption spectrum of **2** using TD-BP86/def2-svp level of theory.

Table S4. TD-DFT calculated electronic transition configuration for **2** along with their corresponding excitation energies, wavelength and oscillator strengths

HOMO is 72

No	Transition configurations (%) ^[a]	Excitation Energy (ev)	Wavelength (nm)		Osc, Strength
			Cal.	Expt.	
1	HOMO→LUMO(99)	2.0880	593.79402		0.0014
2	HOMO-1→LUMO(93)	2.6562	466.7728		0.0041
3	HOMO-2→LUMO(71)	3.0215	410.3398		0.0015
4	HOMO→LUMO+1(26)	3.0713	403.6863	385	0.0134
	HOMO-2→LUMO(21)				
5	HOMO→LUMO+1(70)	3.1620	392.1068		0.0043
	HOMO-3→LUMO(95)				
6	HOMO-4→LUMO(90)	3.4119	363.3875		0.0064
7	HOMO-5→LUMO(54)	3.5335	350.8821		0.0015
	HOMO-1→LUMO+1(32)				
8	HOMO-5→LUMO(17)	3.5665	347.6354		0.0017
	HOMO-1→LUMO+1(43)				
	HOMO→LUMO+2(23)				
9	HOMO-6→LUMO (80)	3.5853	345.8126		0.0044
	HOMO→LUMO+2(16)				
10	HOMO-7→LUMO(20)	3.6337	341.2064	315 ^[b]	0.0065
	HOMO-1→LUMO+1(13)				
	HOMO→LUMO+2(50)				

^[a]components with greater than 10% contribution shown, ^[b]shoulder peak

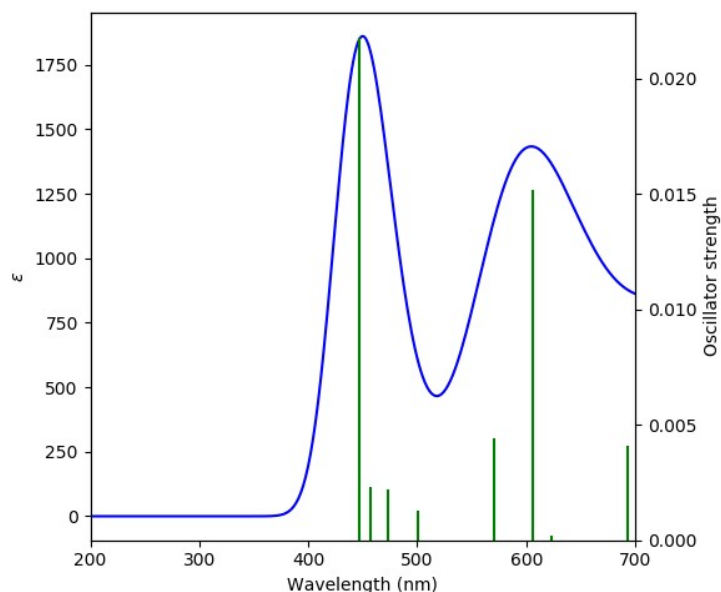


Fig. S42. Calculated absorption spectrum of **3** using TD-BP86/def2-svp level of theory.

Table S5. TD-DFT calculated electronic transition configuration for **3** along with their corresponding excitation energies, wavelength and oscillator strengths

HOMO is 75

No	Transition configurations (%) ^[a]	Excitation Energy (ev)	Wavelength (nm)		Osc, Strength
			Cal.	Expt.	
1	HOMO-2→LUMO(15) HOMO-1→LUMO(84)	1.5660	791.7253		0.0097
2	HOMO-3→LUMO(38) HOMO-2→LUMO(54)	1.7891	692.9975		0.0041
3	HOMO-4→LUMO(88)	1.9909	622.7544		0.0002
4	HOMO-5→LUMO(19) HOMO-4→LUMO(11) HOMO-3→LUMO(45) HOMO-2→LUMO(18)	2.0443	606.4872		0.0152
5	HOMO-5→LUMO(78)	2.1738	570.3569	524	0.0044
6	HOMO-6→LUMO(99)	2.4785	500.2388		0.0013
7	HOMO→LUMO+1(94)	2.6183	473.5293		0.0022
8	HOMO-8→LUMO(39) HOMO-7→LUMO(59)	2.7156	456.5627		0.0023
9	HOMO-8→LUMO(39) HOMO-7→LUMO(38)	2.7730	447.1121	386 ^[b]	0.0218

^[a]components with greater than 10% contribution shown, ^[b]shoulder peak

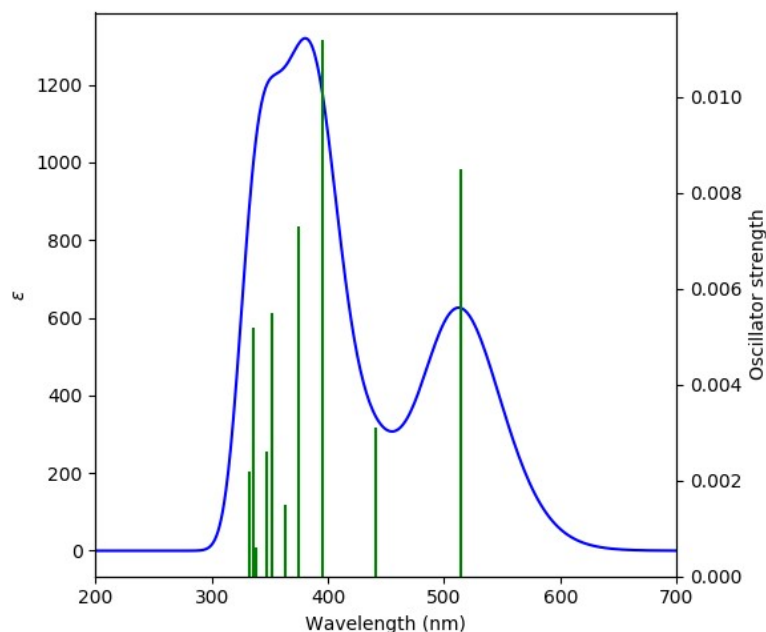


Fig. S43. Calculated absorption spectrum of **4** using TD-BP86/def2-svp level of theory.

Table S6. TD-DFT calculated electronic transition configuration for **4** along with their corresponding excitation energies, wavelength and oscillator strengths

HOMO is 78

No	Transition configurations (%) ^[a]	Excitation Energy (ev)	Wavelength (nm)		Osc, Strength
			Cal.	Expt.	
1	HOMO→LUMO(98)	2.4127	513.8815	514	0.0085
2	HOMO→LUMO+1(99)	2.8108	441.0993		0.0031
3	HOMO-1→LUMO(89)	3.1408	394.7535	394 ^[b]	0.0112
4	HOMO-2→LUMO(89)	3.3095	374.6311	375 ^[b]	0.0073
5	HOMO→LUMO+2(98)	3.4140	363.1640		0.0015
6	HOMO-2→LUMO+1(14) HOMO-1→LUMO+1(80)	3.5263	351.5985		0.0055
7	HOMO-3→LUMO(95)	3.5756	346.7507		0.0026
8	HOMO-4→LUMO(33) HOMO→LUMO+3(65)	3.6640	338.3848		0.0006
9	HOMO-4→LUMO(59) HOMO→LUMO+3(31)	3.6957	335.4822		0.0052
10	HOMO-5→LUMO(61) HOMO-2→LUMO+1(31)	3.7330	332.1301		0.0022

^[a]components with greater than 10% contribution shown, ^[b]shoulder peak

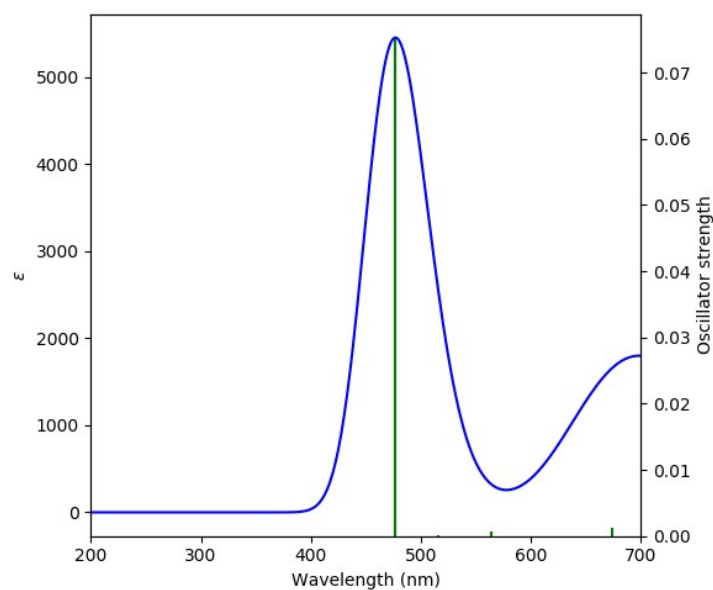


Fig. S44. Calculated absorption spectrum of **5** using TD-BP86/def2-svp level of theory.

Table S7. TD-DFT calculated electronic transition configuration for **5** along with their corresponding excitation energies, wavelength and oscillator strengths

HOMO is 81

No	Transition configurations (%) ^[a]	Excitation Energy (ev)	Wavelength (nm)		Osc, Strength
			Cal.	Expt.	
1	HOMO-2→LUMO(88)	1.7709	700.1196		0.0237
2	HOMO-3→LUMO(99)	1.8396	673.9736		0.0012
3	HOMO-5→LUMO(100)	1.9916	622.5356		0.0
4	HOMO-4→LUMO(82)	2.1972	564.2826		0.0007
5	HOMO-6→LUMO(96)	2.4039	515.7626		0.0002
6	HOMO-7→LUMO(93)	2.4074	515.0128		0.0
7	HOMO-8→LUMO(92)	2.5991	477.0274	448	0.0751
8	HOMO-11→LUMO(97)	2.6447	468.8024		0.0

^[a]components with greater than 10% contribution shown

III Cartesian Coordinates of all Optimized Structures

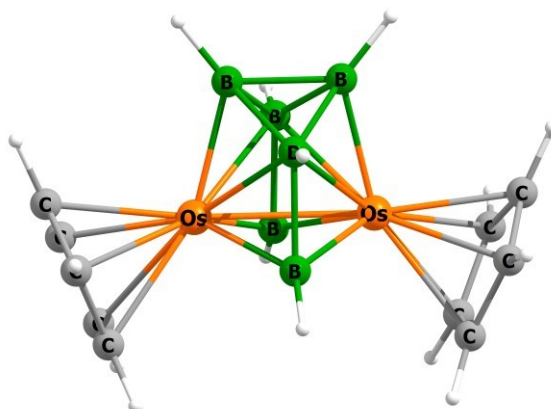


Figure S45. Optimized geometry of **1**.

Total energy = -772.09514246 a.u.

Cartesian coordinates for the calculated structure **1** (in Å)

Os	1.378818000000	0.100903000000	-0.000267000000	H	-1.624418000000	3.146153000000	0.001862000000
Os	-1.378938000000	0.101165000000	-0.000113000000	B	-0.000057000000	-0.434671000000	1.474265000000
C	-3.298763000000	-0.420774000000	1.161105000000	B	0.000129000000	1.362285000000	1.280396000000
C	-3.642335000000	0.360621000000	0.000748000000	H	0.000397000000	1.568227000000	2.483111000000
C	-3.299555000000	-0.419943000000	-1.160484000000	B	-0.000160000000	-0.432799000000	-1.475365000000
C	-2.763569000000	-1.681001000000	-0.715725000000	H	-0.000361000000	-1.101445000000	-2.485327000000
C	-2.763073000000	-1.681518000000	0.715001000000	H	-0.000010000000	-1.104669000000	2.483313000000
C	3.299920000000	-0.419260000000	-1.160210000000	H	2.418703000000	-2.497705000000	1.360850000000
C	3.642045000000	0.361235000000	0.001232000000	H	3.427228000000	-0.110447000000	2.205964000000
C	3.298590000000	-0.420565000000	1.161369000000	H	4.098185000000	1.358416000000	0.002020000000
C	2.763597000000	-1.681445000000	0.714902000000	H	3.429890000000	-0.107889000000	-2.204269000000
C	2.764427000000	-1.680652000000	-0.715813000000	H	2.420349000000	-2.496221000000	-1.363068000000
B	0.872742000000	2.193100000000	0.001059000000	H	-2.418134000000	-2.497529000000	1.361235000000
H	1.624878000000	3.145736000000	0.001615000000	H	-3.427885000000	-0.110482000000	2.205589000000
B	-0.000055000000	1.363949000000	-1.279366000000	H	-4.099015000000	1.357557000000	0.001235000000
H	0.000139000000	1.572783000000	-2.481546000000	H	-3.429460000000	-0.108943000000	-2.204660000000
B	-0.872614000000	2.193259000000	0.001202000000	H	-2.419002000000	-2.496535000000	-1.362762000000

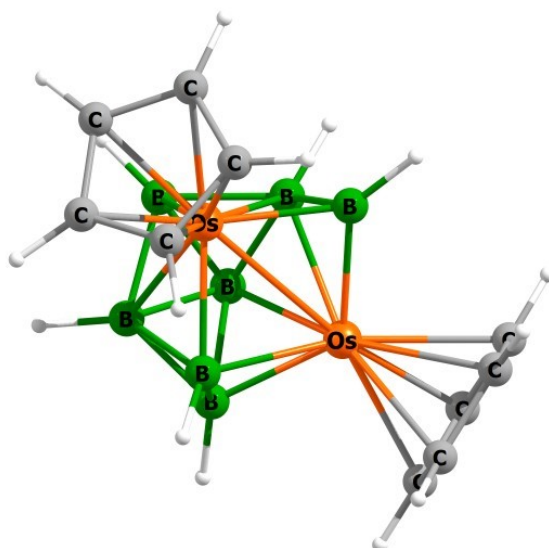


Figure S46. Optimized geometry of **2**.

Total energy = -746.67633018 a.u.

Cartesian coordinates for the calculated structure **2** (in Å)

B	0.120915000000	0.514849000000	1.531500000000	C	2.629309000000	-1.978469000000	-0.013316000000
H	0.192226000000	0.152829000000	2.690751000000	C	-2.783636000000	-1.379690000000	1.195228000000
B	-1.005539000000	1.822816000000	1.103076000000	C	-3.441177000000	-0.107984000000	1.018285000000
H	-1.788745000000	2.450046000000	1.783064000000	C	-3.685321000000	0.088006000000	-0.391482000000
B	-0.655246000000	2.159817000000	-0.632446000000	C	-3.180010000000	-1.067923000000	-1.078327000000
H	-1.314838000000	3.099995000000	-1.035181000000	C	-2.623580000000	-1.966790000000	-0.101733000000
B	-0.081927000000	0.817748000000	-1.603267000000	Os	1.420759000000	0.063944000000	-0.067863000000
H	-0.118414000000	0.675031000000	-2.815117000000	Os	-1.428109000000	0.070731000000	-0.024368000000
B	-0.000542000000	-0.935529000000	-1.186677000000	H	2.342851000000	-1.815629000000	2.223735000000
H	-0.026526000000	-1.901285000000	-1.916700000000	H	3.581661000000	0.593728000000	1.957037000000
B	1.100245000000	1.952785000000	-0.922315000000	H	4.242359000000	0.931863000000	-0.671552000000
H	1.849843000000	2.736571000000	-1.462830000000	H	3.334558000000	-1.251923000000	-2.039249000000
B	0.651689000000	2.091943000000	0.798485000000	H	2.186009000000	-2.953718000000	-0.248459000000
H	1.374052000000	2.934907000000	1.301566000000	H	-2.474192000000	-1.821952000000	2.149778000000
C	3.244501000000	-1.083167000000	-0.958677000000	H	-2.161845000000	-2.939093000000	-0.312414000000
C	3.709460000000	0.074074000000	-0.244546000000	H	-3.201716000000	-1.230073000000	-2.163373000000
C	3.375944000000	-0.116200000000	1.145930000000	H	-4.192450000000	0.946286000000	-0.848885000000
C	2.721969000000	-1.387459000000	1.288206000000	H	-3.718891000000	0.588622000000	1.818224000000

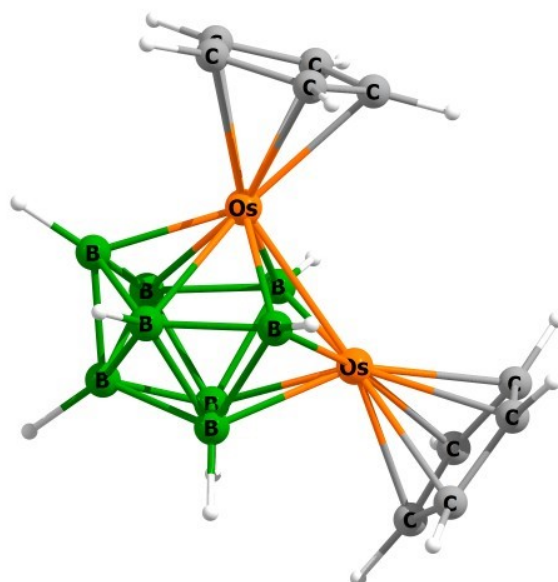


Figure S47. Optimized geometry of **3**.

Total energy = -772.09514246 a.u.

Cartesian coordinates for the calculated structure **3** (in Å)

Os	1.285832000000	-0.095847000000	-0.074398000000	H	-1.506415000000	2.338358000000	-2.316075000000
Os	-1.340053000000	0.033734000000	-0.001747000000	B	0.861937000000	1.840993000000	0.990839000000
C	-2.438329000000	-1.623696000000	-1.189762000000	H	1.776085000000	2.352362000000	1.605217000000
C	-3.416252000000	-0.720097000000	-0.635035000000	B	0.843128000000	1.938212000000	-0.909554000000
C	-3.328383000000	-0.805806000000	0.797468000000	H	1.736989000000	2.545196000000	-1.466038000000
C	-2.305403000000	-1.767472000000	1.129657000000	B	0.072831000000	0.262984000000	1.624758000000
C	-1.766691000000	-2.278348000000	-0.099174000000	H	0.157913000000	-0.299574000000	2.697882000000
C	3.156376000000	-0.590992000000	1.304198000000	B	0.034505000000	0.484300000000	-1.665379000000
C	2.743067000000	-1.778208000000	0.642250000000	H	0.079646000000	0.005048000000	-2.783871000000
C	2.887494000000	-1.560495000000	-0.794750000000	H	-0.974713000000	-3.030669000000	-0.192400000000
C	3.408914000000	-0.245096000000	-1.000454000000	H	-2.001155000000	-2.061191000000	2.140984000000
C	3.518457000000	0.377503000000	0.293857000000	H	-2.242299000000	-1.782450000000	-2.257351000000
B	-1.876162000000	2.073687000000	0.105536000000	H	-3.930156000000	-0.233961000000	1.514565000000
H	-2.980493000000	2.572247000000	0.140762000000	H	-4.099651000000	-0.079073000000	-1.205038000000
B	-0.330366000000	2.877186000000	0.120065000000	H	2.380112000000	-2.695822000000	1.122456000000
H	-0.249424000000	4.086748000000	0.181475000000	H	3.144030000000	-0.411901000000	2.385951000000
B	-0.842916000000	1.787893000000	1.494275000000	H	3.857670000000	1.402722000000	0.482709000000
H	-1.403941000000	2.065215000000	2.535486000000	H	3.631043000000	0.226948000000	-1.964794000000
B	-0.895020000000	1.928038000000	-1.349220000000	H	2.650366000000	-2.289802000000	-1.580998000000

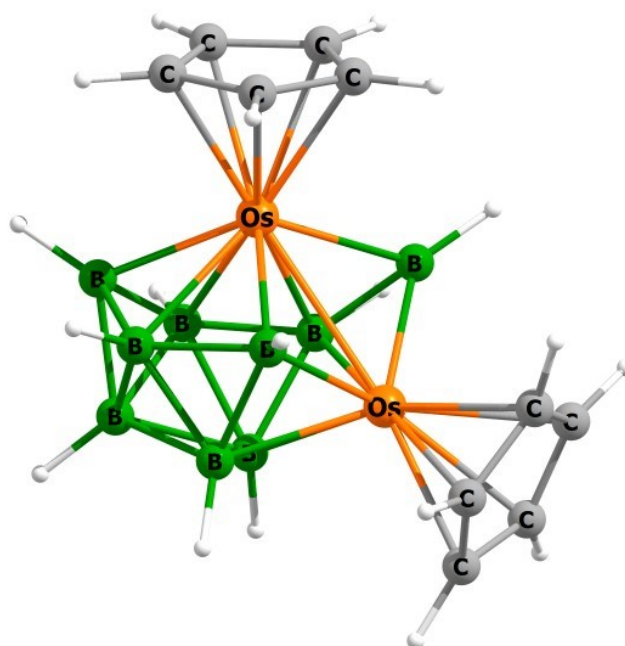


Figure S48. Optimized geometry of **4**.

Total energy = -797.57996987 a.u.

Cartesian coordinates for the calculated structure **4** (in Å)

Os	1.407441000000	-0.038249000000	-0.052697000000	B	-0.873188000000	2.076284000000	-0.829076000000
Os	-1.450091000000	0.015056000000	-0.071903000000	H	-1.664263000000	2.781861000000	-1.422047000000
C	3.565797000000	-0.646178000000	-0.571301000000	B	0.417667000000	2.930064000000	0.142945000000
C	2.718293000000	-1.748718000000	-0.917464000000	H	0.380040000000	4.137923000000	0.254282000000
C	2.092500000000	-2.231554000000	0.295275000000	B	-0.110178000000	0.318519000000	1.537100000000
C	2.550769000000	-1.427417000000	1.387001000000	H	-0.207057000000	-0.233940000000	2.615765000000
C	3.450317000000	-0.434826000000	0.850685000000	B	-0.093120000000	0.707446000000	-1.568985000000
C	-2.618098000000	-1.851271000000	0.746389000000	H	-0.071938000000	0.008075000000	-2.636370000000
C	-3.075760000000	-0.678075000000	1.432382000000	B	-0.129642000000	-0.941353000000	-1.428949000000
C	-3.662087000000	0.211935000000	0.462840000000	H	-0.119861000000	-1.997996000000	-2.013270000000
C	-3.586819000000	-0.421843000000	-0.826975000000	H	2.266207000000	-1.538327000000	2.440057000000
C	-2.933282000000	-1.690907000000	-0.649264000000	H	3.973955000000	0.336251000000	1.428216000000
B	0.967067000000	1.986292000000	-1.324834000000	H	4.186957000000	-0.059980000000	-1.259899000000
H	1.546677000000	2.353886000000	-2.329476000000	H	2.600609000000	-2.179079000000	-1.919225000000
B	1.944192000000	2.098390000000	0.105105000000	H	1.391239000000	-3.072123000000	0.367084000000
H	3.074279000000	2.531342000000	0.155194000000	H	-2.131882000000	-2.719037000000	1.207749000000
B	0.897857000000	1.755253000000	1.430089000000	H	-2.980562000000	-0.480672000000	2.506969000000
H	1.455929000000	1.946398000000	2.494382000000	H	-4.095310000000	1.197938000000	0.670850000000
B	-0.823745000000	1.912584000000	0.977549000000	H	-3.961435000000	-0.006614000000	-1.770964000000
H	-1.659201000000	2.477338000000	1.658407000000	H	-2.737334000000	-2.424813000000	-1.440205000000

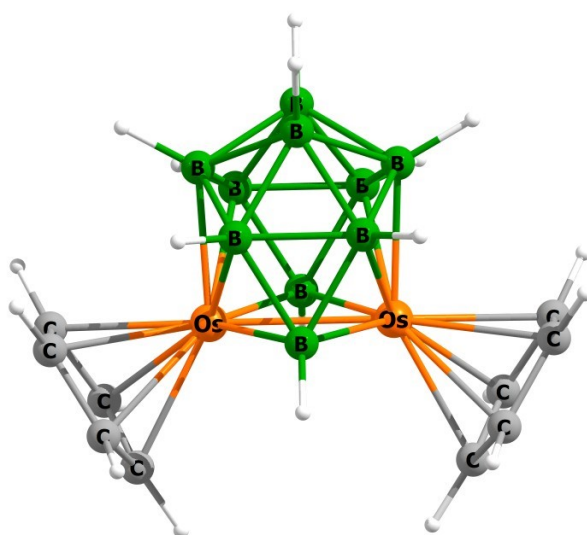


Figure S49. Optimized geometry of **5**.

Total energy = -823.02997392 a.u.

Cartesian coordinates for the calculated structure **3** (in Å)

C	-2.805886000000	-1.446942000000	1.168283000000	H	1.691795000000	1.619274000000	-2.545361000000
C	-2.356473000000	-2.165908000000	0.003978000000	B	0.001570000000	2.813832000000	-0.898990000000
C	-2.802174000000	-1.452997000000	-1.165614000000	H	0.003070000000	3.890297000000	-1.457165000000
C	-3.529620000000	-0.296376000000	-0.720342000000	B	-0.894675000000	1.462987000000	1.641215000000
C	-3.531777000000	-0.292560000000	0.714696000000	H	-1.690699000000	1.621188000000	2.545524000000
C	2.359376000000	-2.164586000000	0.005513000000	B	-0.000796000000	-0.058470000000	1.716888000000
C	2.809231000000	-1.443968000000	1.168732000000	H	-0.001134000000	-0.851073000000	2.637671000000
C	3.532683000000	-0.289073000000	0.713084000000	B	0.895133000000	1.461856000000	1.641637000000
C	3.529153000000	-0.294444000000	-0.721977000000	H	1.691420000000	1.618447000000	2.545981000000
C	2.803281000000	-1.452550000000	-1.165424000000	Os	-1.296389000000	-0.111092000000	-0.000212000000
B	-0.000466000000	-0.058068000000	-1.717105000000	Os	1.295188000000	-0.113273000000	0.000060000000
H	-0.000839000000	-0.850244000000	-2.638233000000	H	3.972503000000	0.471361000000	-1.369254000000
B	-0.894391000000	1.463359000000	-1.641160000000	H	2.616625000000	-1.738634000000	-2.207033000000
H	-1.689999000000	1.621830000000	-2.545779000000	H	1.764480000000	-3.087002000000	0.010531000000
B	-1.399211000000	2.123981000000	0.000063000000	H	2.627564000000	-1.722180000000	2.213358000000
H	-2.455886000000	2.726746000000	-0.000017000000	H	3.979357000000	0.481491000000	1.352374000000
B	0.001342000000	2.813642000000	0.899575000000	H	-1.760550000000	-3.087633000000	0.007420000000
H	0.002645000000	3.890022000000	1.457921000000	H	-2.622863000000	-1.725973000000	2.212450000000
B	1.401489000000	2.122433000000	0.000473000000	H	-3.979300000000	0.476355000000	1.355385000000
H	2.458985000000	2.723538000000	0.000639000000	H	-3.974786000000	0.469339000000	-1.366495000000
B	0.895629000000	1.462159000000	-1.641014000000	H	-2.615978000000	-1.737558000000	-2.207724000000

IV References

- 1 (a) C. L. Gross, S. R. Wilson and G. S. Girolami, *J. Am. Chem. Soc.*, 1994, **116**, 10294; (b) M. I. Bruce, K. Costuas, T. Davin, J.-F. Halet, K. A. Kramarczuk, P. J. Low, B. K. Nicholson, G. J. Perkins, R. L. Roberts, B. W. Skelton, M. E. Smith and A. H. White, *Dalton Trans.*, 2007, 5387.
- 2 (a) J. J. Led and H. Gesmar, *Chem. Rev.*, 1991, **91**, 1413–1426; (b) L. Yang, R. Simionescu, A. Lough and H. Yan, *Dyes Pigm.*, 2011, **91**, 264–267; (c) R. Weiss and R. N. Grimes, *J. Am. Chem. Soc.*, 1978, **100**, 1401–1405.
- 3 (a) G. M. Sheldrick, *Acta Crystallogr., Sect. A: Found. Adv.*, 2015, **A71**, 3–8; (b) G. M. Sheldrick, *SHELXL97*; University of Gottingen: Germany, 1997.
- 4 G. M. Sheldrick, *Acta Crystallogr., Sect. C: Struct. Chem.* 2015, **C71**, 3 – 8.
- 5 O. V. Dolomanov, L. J. Bourhis, R. J. Gildea, J. A. K. Howard and H. Puschmann, *J. Appl. Crystallogr.*, 2009, **42**, 339–341.
- 6 M. J. Frisch, G. W. Trucks, H. B. Schlegel, G. E. Scuseria, M. A. Robb, J. R. Cheeseman, G. Scalmani, V. Barone, B. Mennucci, G. A. Petersson, H. Nakatsuji, M. Caricato, X. Li, H. P. Hratchian, A. F. Izmaylov, J. Bloino, G. Zheng, J. L. Sonnenberg, M. Hada, M. Ehara, K. Toyota, R. Fukuda, J. Hasegawa, M. Ishida, T. Nakajima, Y. Honda, O. Kitao, H. Nakai, T. Vreven, J. A. Montgomery Jr., J. E. Peralta, F. Ogliaro, M. Bearpark, J. J. Heyd, E. Brothers, K. N. Kudin, V. N. Staroverov, R. Kobayashi, J. Normand, K. Raghavachari, A. Rendell, J. C. Burant, S. S. Iyengar, J. Tomasi, M. Cossi, N. Rega, J. M. Millam, M. Klene, J. E. Knox, J. B. Cross, V. Bakken, C. Adamo, J. Jaramillo, R. Gomperts, R. E. Stratmann, O. Yazyev, A. J. Austin, R. Cammi, C. Pomelli, J. W. Ochterski, R. L. Martin, K. Morokuma, V. G. Zakrzewski, G. A. Voth, P. Salvador, J. J. Dannenberg, S. Dapprich, A. D. Daniels, Ö. Farkas, J. B. Foresman, J. V. Ortiz, J. Cioslowski, D. J. Fox, *Gaussian 09, Revision C.01*, Gaussian, Inc., Wallingford, CT, 2010.
- 7 (a) H. L. Schmider, A. D. Becke, *J. Chem. Phys.*, 1998, **108**, 9624–9631; (b) J. P. Perdew, *Phys. Rev. B* 1986, **33**, 8822–8824.
- 8 EMSL Basis Set Exchange Library. <https://bse.pnl.gov/bse/portal>
- 9 (a) E. D. Glendening, A. E. Reed, J. E. Carpenter and F. Weinhold, *NBO Program 3.1*, W. T. Madison, 1988; (b) A. E. Reed, F. Weinhold and L. A. Curtiss, *Chem. Rev.*, 1988, **88**, 899–926; (c) F. Weinhold and R. Landis, *Valency and bonding: A natural bond orbital donor-acceptor perspective*; Cambridge University Press: Cambridge, U.K, 2005.
- 10 K. Wiberg, *Tetrahedron*, 1968, **24**, 1083–1096.
- 11 I. I. Dennington, R. T. Keith, J. Millam, K. Eppinnett, W. L. Hovell and R. Gilliland, *GaussView, Version 3.09*; Semichem Inc.: Shawnee Mission, KS, 2003.
- 12 G. A. Zhurko, <http://www.chemcraftprog.com>